PSBench: a large-scale benchmark for estimating the accuracy of protein complex structural models

Pawan Neupane*
University of Missouri - Columbia
pngkg@missouri.edu

Jian Liu*
University of Missouri - Columbia
jl4mc@missouri.edu

Jianlin Cheng†
University of Missouri - Columbia
chengji@missouri.edu

Abstract

Predicting protein complex structures is essential for protein function analysis, protein design, and drug discovery. While AI methods like AlphaFold can predict accurate structural models for many protein complexes, reliably estimating the quality of these predicted models (estimation of model accuracy, or EMA) for model ranking and selection remains a major challenge. A key barrier to developing effective machine learning-based EMA methods is the lack of large, diverse, and well-annotated datasets for training and evaluation. To address this gap, we introduce PSBench, a benchmark suite comprising five large-scale, labeled datasets, four of which were generated during the 15th and 16th community-wide Critical Assessment of Protein Structure Prediction (CASP15 and CASP16), and one curated for new Protein Data Bank (PDB) entries deposited between July 2024 and August 2025. PSBench includes over 1.4 million structural models covering a wide range of protein sequence lengths, complex stoichiometries, functional classes, and modeling difficulties. Each model is annotated with multiple complementary quality scores at the global, local, and interface levels. PSBench also provides multiple evaluation metrics and baseline EMA methods to facilitate rigorous comparisons. To demonstrate PSBench's utility, we trained and evaluated GATE, a graph transformer-based EMA method, on the CASP15 data. GATE was blindly tested in CASP16 (2024), where it ranked among the top-performing EMA methods. These results highlight PSBench as a valuable resource for advancing EMA research in protein complex modeling. PSBench is publicly available at: `https://github.com/BioinfoMachineLearning/PSBench`.

1 Introduction

Proteins are essential biological macromolecules whose diverse functions in living organisms are dictated by their three-dimensional (3D) structures. Although experimental techniques such as X-ray crystallography, cryo-electron microscopy (cryo-EM), and nuclear magnetic resonance (NMR) spectroscopy can determine protein structures with high accuracy, these approaches are time-consuming and resource-intensive and can only be applied to a tiny portion ($< 0.1\%$) of proteins.

To overcome these challenges, machine learning methods[1, 2, 3, 4, 5, 6, 7, 8, 9] for predicting protein structures from sequences have become essential. Among these, AlphaFold[1, 10, 11] has

[*] Equal contribution.

[†] Corresponding author.

39th Conference on Neural Information Processing Systems (NeurIPS 2025) Track on Datasets and Benchmarks.

revolutionized the field by achieving experimental accuracy for predicting the tertiary structures of almost all single-chain proteins (monomers) first and then delivering high-accuracy structure prediction for a large portion of multi-chain protein complexes (multimers). As monomer structure prediction is largely considered solved, protein complex structure prediction is currently one major focus in the field. Despite its success, a critical limitation persists: AlphaFold's self-estimated model accuracy (quality) scores (e.g., plDDT, pTM, ipTM, and confidence scores) are not always reliable for identifying high-quality predicted complex structures (structural models)[12]. For instance, using AlphaFold2-Multimer or AlphaFold3 to predict many (e.g., thousands of) structural models for a protein complex target can substantially increase the likelihood of generating some high-quality ones[9], but AlphaFold's own confidence scores or ranking scores often cannot rank them at the top when the ratio of high quality models versus low-quality models is low. As a result, selecting structural models of high quality from a pool of models generated by AlphaFold or other AI methods is a major challenge in protein complex structure prediction and sometimes even harder for users than model generation itself[8].

This challenge highlights the importance of Estimation of Model Accuracy (EMA) (also called model quality assessment), which predicts how closely a predicted structural model resembles the native (true) structure before the true structure is known. Reliable EMA tools are not only critical for model selection in the prediction phase, but also vital to prioritize accurate structural models for downstream applications such as protein function annotations and drug discovery. To stimulate the development of EMA methods for protein complex structural models, since 2020, CASP has dedicated one competition category to assess EMA methods[13, 14]. However, EMA methods remain underdeveloped due to two critical gaps: the lack of large, high-quality, labeled complex model datasets to train and test machine learning EMA methods (like ImageNet for image processing) and the lack of user-friendly standardized benchmarks and automated evaluation tools to assess the performance of EMA methods.

To bridge this gap, we introduce PSBench, a comprehensive benchmark for training and testing EMA methods to predict the accuracy (quality) of predicted protein complex structural models and comparing them with baseline methods via multiple complementary metrics (Fig. 1). PSBench consists of five complex structure datasets, including four datasets with more than one million community-predicted and in-house-predicted structures for protein complex targets of the 2022 CASP15[14, 15, 16] and 2024 CASP16 competitions[17], and a newly curated dataset of AlphaFold3-predicted models for the PDB entries deposited between July 2024 and August 2025. The CASP-related datasets were generated in the truly blind prediction setting (e.g., true structures were unavailable during prediction). These structural models were predicted mainly by AlphaFold2-Multimer[10] and AlphaFold3[11] for 79 diverse, representative protein complex targets with different lengths, difficulties and stoichiometries (count of each unique chain in a protein complex), carefully selected by protein structure experts[15]. The newly curated dataset further expands this diversity by adding 400,400 structural models for 2,002 targets, increasing the total number of complex targets to 2,081. Each model is rigorously labeled with 10 distinct quality scores spanning global, local and interface accuracy measures (Fig. 1a). Importantly, CASP15 models and CASP16 models were generated two years apart and therefore can provide a rigorous split of data for training and testing EMA methods, preventing information leakage and mirroring real-world EMA workflows.

To demonstrate PSBench can be used to train advanced EMA methods and rigorously benchmark them prior to their use, we trained and tested GATE[18], a graph transformer-based EMA method on two CASP15 datasets (CASP15_inhouse_dataset and CASP15_community_dataset) respectively for two purposes: (1) estimating the accuracy of structural models generated by one predictor for model selection and ranking, a typical setting for structure predictors and users; and (2) estimating the accuracy of structural models generated by many predictors in a community, which is a typical setting of CASP EMA competition. We then blindly tested two GATE variants in the blind CASP16 competition held from May to August 2024.

In the official CASP16 EMA competition category, GATE ranked among the best methods out of 38 participating EMA predictors. In the blind ranking and selection of in-house structural models predicted by our own protein structure system (MULTICOM4) built on top of AlphaFold2-Multimer and AlphaFold3 during CASP16, GATE also outperformed five standard EMA methods and helped MULTICOM4 rank among top predictors in protein complex structure prediction in CASP16[9]. The results demonstrate that PSBench is a valuable resource, including labeled datasets, a model annotation pipeline, baseline EMA methods, and evaluation tools/metrics, for the AI community to develop and benchmark cutting-edge machine learning methods to estimate protein complex model accuracy, addressing a significant bottleneck in the field of protein structure prediction.

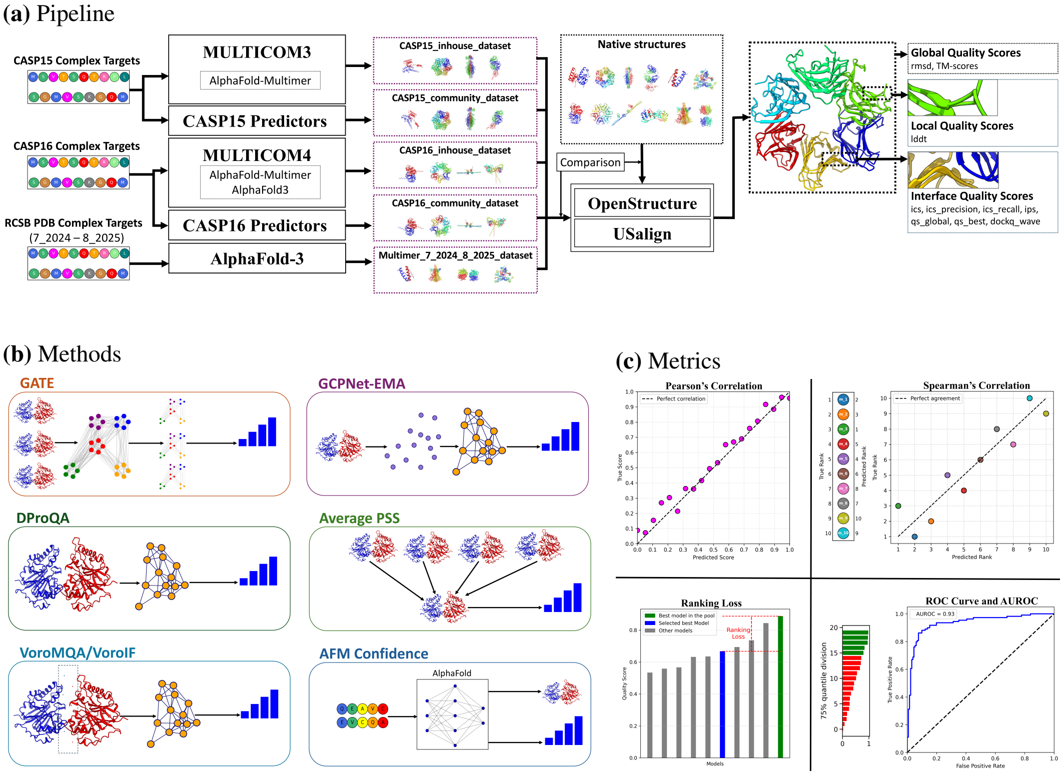

Figure 1: Overview of PSBench. (a) Pipeline. The PSBench pipeline for preparing five datasets for estimating protein complex model accuracy (EMA). The predicted structural models are compared with native (true) structures to compute global, local, interface quality scores as labels. **(b) Methods.** Six representative baseline EMA methods for performance comparison. **(c) Metrics.** Four metrics for evaluating EMA methods: Pearson's correlation, Spearman's correlation, ranking loss, and AUROC (Area Under Receiver Operating Characteristics Curve) for evaluating predicted model quality scores against true ones (labels). The evaluation tools are included in PSBench.

2 Background and Related Work

The development of EMA methods, either physics-/statistical potential-based methods[19, 20] or data-driven machine learning methods[21, 22, 23], requires the availability of high-quality datasets of predicted protein complex structural models with annotated quality scores. Particularly, the recently emerged, more powerful deep learning-based EMA methods need to be trained and tested on large, diverse structural model datasets to reliably predict the accuracy (quality) of structural models sampled from the vast protein structure space.

Early benchmark datasets, such as the Docking Benchmark (BM)[24], PPI4DOCK[25], and DockGround[26], consist of structural models generated by traditional protein docking tools like SwarmDock[27], ZDock[28], and pyDock[29]. However, as docking tools are not accurate and have been largely replaced by much more accurate AlphaFold, these datasets are not suitable for training machine learning methods to predict the quality of structural models generated by widely used AlphaFold. Moreover, these datasets are relatively small. For instance, PPI4DOCK has 54,000 structural models, and CAPRI Score_set[30] comprises 19,013 structural models for 15 targets. Furthermore, the structural models were mostly predicted for small protein complexes (such as homo- and hetero-dimers), which cannot represent large protein complexes consisting of many chains and having more complicated stoichiometries.

Recent efforts have sought to apply state-of-the-art protein complex structure predictors like AlphaFold2 and AlphaFold2-Multimer to create benchmark datasets. For instance, Multimer-AF2 Dataset (MAF2)[31] comprises 9,251 structural models generated by AlphaFold2 and AlphaFold2-Multimer, while Heterodimer-AF2 Dataset (HAF2)[31] is a collection of 1,849 structural models for 13 heterodimer proteins generated by the same tools. These datasets have enabled the development of advanced EMA methods such as DProQA[31] and ComplexQA[32]. However, like the early datasets, these datasets contain a small number of structural models generated for small to medium protein complexes (e.g., sequence length less than 1500 residues), and therefore cannot represent the diverse protein complex structure space well. Moreover, both early and recent benchmark datasets have a limited set of quality scores assigned to each structural model without capturing different aspects of model quality. And the structural models in these datasets were generated in a simulated prediction environment where true structures were known, which is different from the truly blind prediction setting where structural models are predicted prior to true structures being available.

Finally, the previous benchmarks do not provide automated evaluation tools and baseline methods to benchmark new EMA methods, which are important for speeding up the development of machine learning EMA methods. And they do not include tools to automatically annotate and incorporate new structural models so that they cannot be expanded.

To address the gaps above, we develop PSBench, a large, comprehensive benchmark for developing, training, and testing EMA methods for protein complex. PSBench makes the following unique contributions to the field.

- Providing more than 1.4 million complex structural models generated by state-of-the-art deep learning methods (mostly AlphaFold2-Multimer and AlphaFold3), much larger than previous datasets.
- Four of the five datasets (about 1 million models) were generated in the real-world blind prediction setting (CASP15 and CASP16 competitions) without any knowledge of true structures. In addition, a newly curated dataset of AlphaFold3-predicted models for protein complexes deposited in the PDB between July 2024 and August 2025 enables continuous benchmarking with recent structural data.
- The structural models were generated for 2,081 diverse protein complex targets including 79 CASP ones carefully selected by protein structure experts, encompassing 185 distinct stoichiometries, multiple functional classes, varying difficulty levels (easy, medium, and hard), and a wide range of sequence lengths (12 to 8,460 residues).
- The structural models are assigned 10 complementary quality scores at the local, global, and interface levels, measuring their accuracy from different perspectives, important for training and evaluating EMA methods.
- Providing automated evaluation tools for comparing new EMA methods with 6 standard baseline EMA methods, as well as a model annotation (labeling) pipeline for continuous expansion of the datasets.
- The utility of PSBench for developing state-of-the-art EMA methods was blindly and rigorously proved in CASP16.

3 PSBench Design

PSBench encompasses over 1.4 million predicted structural models, distributed across five datasets: CASP15_inhouse_dataset, CASP15_community_dataset, CASP16_inhouse_dataset, CASP16_community_datase, and Multimer_7_2024_8_2025_dataset. The first four datasets were generated for 79 CASP complex targets during the 2022 CASP15 competition and the 2024 CASP16 competition, while the fifth dataset consists of AlphaFold3-generated structural models for 2,002 non-redundant multimeric protein entries deposited in the RCSB PDB between July 2024 and August 2025 (Fig. 1a).These targets represent 185 distinct stoichiometries (Fig. S1a in Appendix A.1) and more than 145 protein classes (Fig. S1b), providing a broad coverage of protein complexes.

The structural models were compared with the corresponding native (true) structures of the targets by an automated annotation pipeline in PSBench to assign quality scores to them as labels. The annotation pipeline pre-processed structural models and true structures so that they could be aligned and compared by two tools, OpenStructure[33, 34, 35] and USalign[36], generating 10 complementary quality scores measuring model accuracy from three different aspects: global quality, interface quality, and local quality (see the detailed description of these quality scores in Appendix A.2). The global quality scores (variants of `tm-score` and `rmsd`) quantify the similarity between the global fold of a model and that of the true structure. The interface quality scores (`ics`, `ics_precision`,`ics_recall`, `ips`, `qs_global`, `qs_best`, and `dockq_wave`) measure the quality of interface regions where two chains in a protein complex interact. The local quality score (`lddt`) measures the accuracy of the location of each residue with respect to its contacted residues.

The quality scores computed by the annotation pipeline for the models in the CASP15_community_dataset and CASP16_community_dataset were cross-validated with the scores compiled from the CASP15 and CASP16 websites to make sure that it worked correctly (see Appendix A.3 for preprocessing, implementation details and edge cases). Users can use one or more quality scores to train and test their EMA methods. Generally, it is recommended at least one global quality score and one interface quality score be used to benchmark EMA methods. We also analyzed inter-score relationships and redundancy (Appendix A.4) and examined how the interface contact density relates to interface quality scores (Appendix A.5). A detailed guidance linking each quality score to relevant structural biology and bioinformatics applications is presented in Appendix A.6. The main characteristics of the five datasets are discussed below.

3.1 CASP15_inhouse_dataset

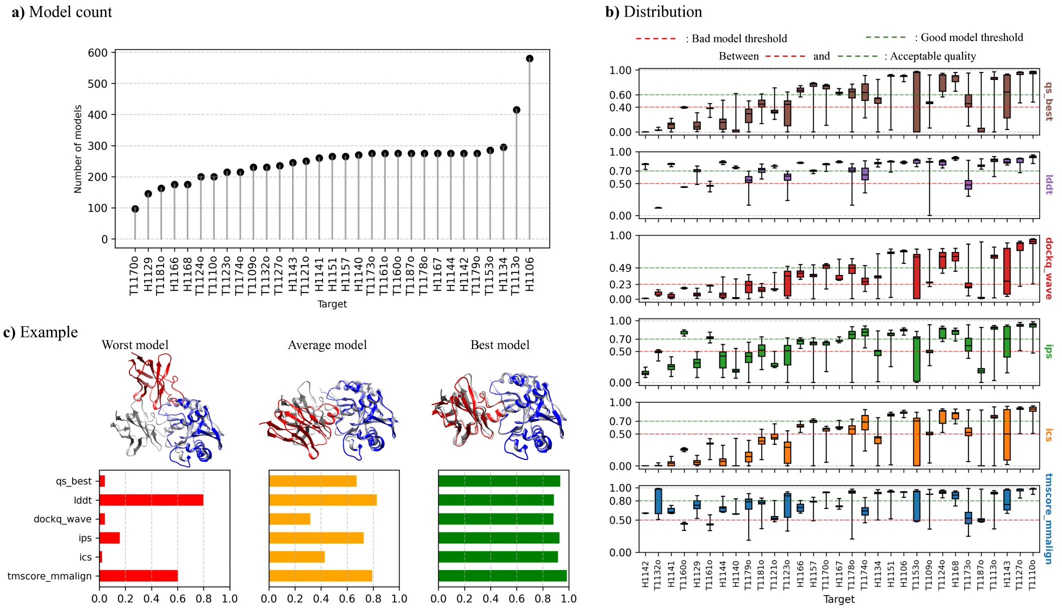

Figure 2: CASP15_inhouse_dataset. (a) Model count. Number of models per target in the dataset. **(b) Score Distribution.** Box plots of each of six representative quality scores of the models for each target. **(c) Example.** Three representative models (worst, average, best) in terms of sum of the six representative quality scores for a target H1143. Each model with two chains colored in blue and red is superimposed with the true structure in gray.

The structural models in CASP15_inhouse_dataset were generated by our MULTICOM3[8] system during the 2022 CASP15 competition. MULTICOM3 generated diverse multiple sequence alignment (MSA), structural templates and hyperparameters as input for AlphaFold2-Multimer[10] to predict the structures for 31 CASP15 complex targets and ranked as one of top 10 complex predictors in CASP15. It generated 97 to 580 structural models per target (see model count per target in Fig. 2a), resulting in 7,885 models in total included in CASP15_inhouse_dataset.

The 31 CASP15 targets cover a wide range of distinct stoichiometries, sequence lengths, protein classes (see Table S1 for details). The distribution of six representative quality scores of the structural models for the targets are visualized as box plots in Fig. 2b. It can be seen that the targets are of different difficulty levels. Some easy targets have most models above the threshold of good quality, some average targets have one portion of models above the good model threshold and another portion below the bad model threshold, and some difficult targets have most models below the bad model threshold. Therefore, this dataset is ideal for benchmarking EMA methods' capability to work for different kinds of targets and train them to possess the capability. The detailed numbers of good, acceptable, and bad models are reported in Table S2. Fig. 2c illustrates three representative models (worst, average, and best) of a target H1143 and their quality scores.

Because the structural models in CASP15_inhouse_dataset were generated by our own predictor, in addition to a structural file in the Protein Data Bank (PDB) format, every model has four extra features, i.e., four estimated quality scores assigned by AlphaFold2-Multimer during the model generation process, including AlphaFold2-Multimer confidence score (`afm_confidence_score`), interface predicted Template Modeling score (`iptm`), number of inter-chain predicted aligned errors (<5 Å) (`num_inter_pae`), and predicted multimer DockQ score (`mpDockQ`) (see Appendix A.7 for details). This is different from CASP15_community_dataset generated by many CASP15 predictors that did not submit these features. It is worth noting that these estimated model quality scores are not true quality scores, but can be used as input features to improve the prediction of true quality scores[18]. Therefore, CASP15_inhouse_dataset is an excellent resource for training EMA methods to rank and select structural models generated by AlphaFold-based structure predictors.

3.2 CASP15_community_dataset

The CASP15_community_dataset contains structural models submitted by 87 predictors during the CASP15 competition, where each predictor submitted at most 5 models for each target. Most predictors used different variants of AlphaFold2 and AlphaFold2-Multimer to generate models, while some predictors also used other structure prediction methods such as template-based modeling and protein language model-based modeling (e.g., ESMFold[37]), resulting in a diverse set of structural models. It contains 215 to 319 structural models per target and 10,942 models in total for 40 complex targets (see model count per target in Fig. S5a and Table S3).

Unlike CASP15_inhouse_dataset generated in an in-house controlled generation process, CASP15_community_dataset has more variability in modeling approaches and model quality. As shown in Fig. S5b, the quality scores of the models for many targets spread in a wider range, making the dataset particularly valuable for training and benchmark EMA methods for estimating the accuracy of the models generated by a diverse set of predictors with different performance. Fig. S5c illustrates three representative models for a target. Table S4 reports the number of bad, acceptable and good models for each target. Some targets such as T1160o have only one or a few good models, making them challenging targets for EMA methods to pick good ones.

3.3 CASP16_inhouse_dataset

The structural models in CASP16_inhouse_dataset were generated by our MULTICOM4 system[9] built on top of both AlphaFold2-Multimer and AlphaFold3[11] during 2024 CASP16 competition. MULTICOM4 ranked no. 1 in the Phase 0 competition of CASP16 in which the stoichiometry of each target was not provided and needed to be predicted and among top 5 in the Phase 1 competition in which the stoichiometry was provided. MULTICOM4 generated 712 to 78,410 structural models for each target (see model count per target in Fig. S6a), resulting in 1,009,050 models for 36 complex targets. The stoichiometry, total number of models, number of AlphaFold3 models, sequence length, and protein class for each target are reported in Table S5. The CASP16 targets represent a broad range of stoichiometries, protein classes, and sequence lengths.

Fig. S6b illustrates the distribution of the six representative quality scores of the models across targets. In contrast to CASP15_inhouse_dataset, CASP16_inhouse_dataset exhibits greater variability in model quality, due to a much larger number of models per target and the use of both AlphaFold2-Multimer and AlphaFold3. Table S6 reports the number of good, acceptable, and bad models for each target. Some targets have many good models, while other have very few, representing different levels of difficulty. As an example, the worst, average, and best models of target T1235o are shown in Fig. S6c.

Same as CASP15_inhouse_dataset, each model in CASP16_inhouse_dataset also includes four AlphaFold2-Multimer-like self-estimated quality features. Additionally, AlphaFold3-based models have one more feature, `af3_ranking_score`. These scores can be used as input features for EMA methods to predict the quality of the models. Due to these additional features and a very large number of structural models for a diverse set of protein complex targets, CASP16_inhouse_dataset is a large, valuable resource to train and benchmark EMA to estimate the accuracy of structural models predicted by both AlphaFold2-Multimer and AlphaFold3. Particularly, to our knowledge, it contains the largest number of labeled protein complex structural models generated by AlphaFold3 to date.

3.4 CASP16_community_dataset

CASP16_community_dataset comprises 12,904 models for 39 complex targets (166 to 377 models per target) generated by 82 predictors during the CASP16 competition. Most of the predictors used AlphaFold2-Multimer and/or AlphaFold3 to generate structural models, even though some predictors used additional prediction techniques. The per-target model counts, distribution of quality scores and three model examples are illustrated in Fig. S9. The stoichiometry, protein class, sequence length, and number of good/acceptable/bad models of each target are reported in Tables S7 and S8.

Like CASP15_community_dataset, the models in CASP16_community_dataset originated from a large number of diverse predictors and therefore have a wide range of quality scores (Fig. S9b). The dataset is ideal for training and benchmarking EMA methods for predicting the quality of structural models generated by various modern deep learning-based protein structure prediction methods including, but not limited to AlphaFold2-Multimer and AlphaFold3.

3.5 Multimer_7_2024_8_2025_dataset

Multimer_7_2024_8_2025_dataset expands the CASP datasets by including 400,400 AlphaFold3-predicted models (200 per target) for 2,002 non-redundant multimeric protein entries deposited in the RCSB PDB between July 2024 and August 2025. Initially, 3,379 targets were collected from the PDB and subjected to redundancy reduction by grouping entries that contain the same number of protein chains with identical sequences but differ in ligands or nucleic acids, followed by selection of representative targets (i.e. the target in each group that appeared first in the PDB). This process yielded 2,216 unique entries for AlphaFold3 prediction, of which 214 could not be processed due to GPU memory constraints arising from large residue count. It is worth noting that the PDB is continuously updated, and the exact number of available entries within a deposition window may vary over time.

This dataset represents the most diverse collection in PSBench, encompassing 179 distinct stoichiometries and 143 distinct protein classes. The lengths of the targets range from 12 to 4,591 residues (see Fig. S10). The distribution of average structural quality scores across all targets in the `Multimer_7_2024_8_2025_dataset` is shown in Fig. S11.

Similar to the in-house datasets, each model in `Multimer_7_2024_8_2025_dataset` contains AlphaFold-derived self-estimated features, including `afm_confidence_score` (Fig. S12), `af3_ranking_score` (Fig. S13), `iptm`, `num_inter_pae`, and `mpDockQ`. These features can be used as input for EMA methods to predict structural accuracy.

4 Evaluation Framework

4.1 Evaluating the Utility of PSBench for Training and Testing EMA Methods

To assess if PSBench could support the development of machine learning EMA methods, we trained and validated a graph transformer EMA method (GATE[18]) on CASP15_inhouse_dataset and CASP15_community_dataset separately to obtain two EMA predictors, i.e., (1) one (referred to as GATE-AFM) for predicting the quality scores of structural models generated by AlphaFold and (2) another (referred to as GATE) for predicting the quality scores of structural models generated by many predictors participating in CASP. The two predictors were blindly tested during the CASP16 competition from May to August 2024 as follows.

First, GATE-AFM was used to predict the quality of the in-house structural models generated by MULTICOM4 and select top ones to submit to CASP16 for complex structure prediction competition. To benchmark how GATE performed, five standard EMA methods with source codes available were blindly run in parallel during CASP16, which included DProQA[31], VoroIF-GNN scores[38], GCPNet-EMA[39], PSS[40] and AlphaFold2-Multimer confidence scores (AFM Confidence) (Fig.

1b) (see Appendix B.1 for details). The model quality scores predicted by GATE-AFM and the five methods were compared with the true quality scores available only after CASP16 concluded in December 2024 (see the results in Section 5.1). The six methods are included in PSBench for comparison with future EMA methods.

Second, GATE directly participated in the EMA competition category of CASP16 to evaluate the complex structural models generated by CASP16 complex structure predictors. GATE was assessed along with 37 EMA predictors participated in the CASP16 EMA competition by CASP16 organizers and assessors (see the results in Section 5.2). This assessment is highly rigorous and objective because GATE was evaluated with the best EMA predictors in the field by external experts.

4.2 Protocols of Training and Validating GATE-AFM and GATE on CASP15 Datasets

GATE-AFM and GATE use the same graph transformer architecture to predict the global quality scores of structural models. It takes as input a graph of a set of structural models of a target, in which a node denotes a model and an edge connects two similar models, to predict the quality score (e.g., TM-score) of each model. The common features for each node shared by both GATE-AFM and GATE are the estimated model quality scores assigned by several EMA methods. The only difference between GATE-AFM and GATE is that the former uses four additional AlphaFold2-Multimer features (confidence scores, ipTM, number of inter-chain predicted aligned errors and mpDockQ) that are only available in CASP15_inhouse_dataset but not in CASP15_community_dataset. GATE-AFM and GATE use the same set of edge features, including structural similarity scores between two connected nodes.

GATE was trained and validated on the CASP15_community_dataset via 10-fold cross-validation, which comprises 10,935 models of 40 complex targets, plus 187 models from another target (i.e., T1115o) whose native structure is not publicly available. For this target, we obtained its quality scores from the CASP15's website as labels. For each target, a pairwise similarity graph was constructed for all the models of each target first. 2000 subgraphs containing up to 50 nodes were then sampled from the full graph of each target to train and validate GATE. GATE-AFM was trained and validated on the CASP15_inhouse_dataset in the similar way. To reduce computational costs, only a subset of CASP15_inhouse_dataset was used to train GATE-AFM (see Appendix A.13). The details of training and validation are provided in the Appendix B.2, and a discussion of computational requirements is included in Appendix B.3.

4.3 Evaluation Metrics

PSBench provides four complementary metrics (Fig. 1c) to evaluate the performance of EMA methods. Pearson's correlation coefficient measures the linear correlation between predicted quality scores from an EMA method and ground-truth quality scores. Spearman's correlation coefficient evaluates rank-order consistency between predicted scores and ground-truth scores. Ranking loss directly assesses model selection capability by computing the difference between the ground-truth quality score of the truly best model (highest ground-truth score) and the ground truth score of the no.1 model selected by an EMA method, where lower loss values correspond to better selection and 0 means a prefect selection. Area Under the Receiver Operating Characteristic Curve (AUROC) quantifies binary classification performance by labeling models as high-quality (above the 75th percentile of ground-truth scores) or low-quality otherwise. An AUROC of 1.0 indicates perfect classification, while 0.5 corresponds to random guessing. Each metrics is usually calculated for the models of each protein target first and then is averaged over all the targets in a dataset as the performance score for an EMA method. The scripts that can automatically calculate these scoring metrics for EMA methods are included in PSBench.

5 Results

5.1 Blind Prediction Results of Estimating the Accuracy of CASP16 In-house Models

During CASP16 competition, GATE-AFM pretrained on a subset of CASP15_inhouse_dataset, was blindly applied to our in-house models generated by MULTICOM4. Due to the three-day prediction time constraint, we used it to predict the quality of only hundreds of top-ranked models for each target (i.e., the collection of top 5 models generated by each of dozens of predictors based on AlphaFold2-

Multimer and AlphaFold3 in MULTICOM4). Four targets (T1249v1o and T1249v2o, T1294v1o and T1294v2o) that have the same sequence but different conformations are excluded. The performance of GATE and the other EMA methods on the top models for the remaining 32 targets (referred to as CASP16_inhouse_TOP5_dataset, a subset of CASP16_inhouse_dataset) was compared in Table 1.

Table 1: Performance of EMA methods in estimating the accuracy of the CASP16 in-house models. Metrics include Pearson's correlation (Corr^{P}), Spearman's correlation (Corr^{S}), ranking loss, and AUROC, reported separately for TM-score and DockQ_wave. Bold font and underline denote the best and second best results respectively. Significant difference ($p < 0.05$) between GATE-AFM and other methods based on the one-sided Wilcoxon signed-rank test is marked with *.

Method	TM-score				DockQ_wave			
	Corr^{P} ↑	Corr^{S} ↑	Loss ↓	AUROC ↑	Corr^{P} ↑	Corr^{S} ↑	Loss ↓	AUROC ↑
GATE-AFM	0.372	**0.283**	**0.102**	**0.658**	**0.431**	**0.322**	**0.138**	**0.662**
AFM Confidence	0.259*	0.143*	0.106	0.597*	0.252*	0.114*	0.151	0.593*
PSS	**0.394**	0.261	0.114	0.647	0.369	0.284	0.154	0.645
GCPNet-EMA	0.360	0.249	0.135	0.643	0.355	0.264	0.169	0.648
VoroMQA-dark	0.039*	0.144	0.129	0.609	-0.013*	0.146*	0.163	0.622
VoroIF-GNN-pCAD-score	0.073*	0.105*	0.167*	0.589*	0.074*	0.137*	0.204	0.615
VoroIF-GNN-score	0.065*	0.116*	0.193*	0.599*	0.114*	0.170*	0.207*	0.622
DProQA	-0.051*	0.011*	0.194*	0.569*	0.032*	0.071*	0.223*	0.587*

GATE-AFM outperformed the other methods according to almost all evaluation metrics. In terms of a global quality score - TM-score, GATE-AFM achieved the highest Spearman's correlation (0.283), the lowest ranking loss (0.102), the best AUROC (0.658), and second highest Pearson's correlation (0.372), indicating superior ranking consistency and classification reliability. In terms of an interface quality score - DockQ_wave, GATE-AFM again outperformed all other methods, attaining the highest Pearson's correlation (0.431), the highest Spearman's correlation (0.322), the lowest ranking loss (0.138), and the highest AUROC (0.662). It performed better than AFM Confidence (the default self-estimated quality score of AlphaFold2-Multimer) in terms of all the metrics, demonstrating its significant value of estimating the quality of AlphaFold-generated structural models. In many cases, the improvement of GATE-AFM over the other methods is significant (see the cases marked with * in Table 1). Additional AUROC analyses with fixed thresholds (e.g., TM-score ≥ 0.5, DockQ_Wave ≥ 0.49) are provided in Appendix B.4. To complement these aggregate results, we also examined some failed cases with large prediction errors, which revealed two distinct failure modes (Appendix B.5). GATE-AFM's strong capability of selecting good models was one important reason that our MULTICOM4 predictors ranked among top predictors in the CASP16 complex structure prediction category[9]. These results show that PSBench can be used to develop state-of-the-art EMA methods.

5.2 Blind Prediction Results in CASP16 EMA Competition

GATE, pretrained on CASP15_community_dataset, participated in 2024 CASP16 EMA competition under the predictor name: MULTICOM_GATE. We downloaded the EMA prediction results of MULTICOM_GATE and other 37 CASP16 EMA predictors from the CASP16 website. Two very large targets (H1217 and H1227) were excluded because GATE did not generate predictions for their models due to time constraints during CASP16, resulting in using 37 out of 39 targets in CASP16_community_dataset for evaluation.

The blind prediction results of top 20 out of 38 CASP16 EMA predictors were shown in Fig. 3. In terms of TM-score, MULTICOM_GATE was ranked first according to Pearson's correlation (0.673), third according to Spearmans' correlation (0.456), ranking loss (0.135) and AUROC (0.652) respectively. Moreover, we assessed the performance of the 38 EMA predictors using a Z-score–based ranking, where MULTICOM_GATE ranked third (see detailed results in Appendix B.6). The outstanding performance of MULTICOM_GATE in CASP16 EMA competition[41] highlights PSBench's unique value: its high-quality training and test datasets and rigorous evaluation protocols provide a strong framework to develop and validate state-of-the-art machine learning methods.

6 Conclusion, Limitations and Future Work

PSBench fills critical gaps in protein complex model accuracy estimation by providing a large-scale benchmark with both data and tools for training and testing EMA methods. It contains more than one million labeled structural models for 79 CASP15/16 targets that cover diverse stoichiometries, function classes, sequence lengths, and difficulty levels. PSBench's value of supporting the development of generalizable EMA methods has been demonstrated by the outstanding performance of GATE trained with it in the blind community-wide CASP16 competition in 2024.

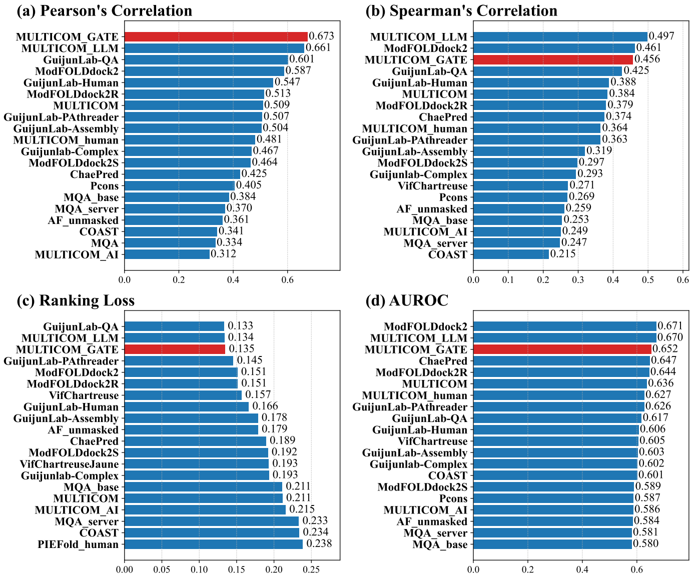

Figure 3: CASP16 EMA results. The performance of top 20 out of 38 CASP16 EMA predictors in predicting TM-scores of structural models of 37 complex targets. **(a)** Pearson's correlation. **(b)** Spearman's correlation. **(c)** Ranking loss. **(d)** AUROC. MULTICOM_GATE is highlighted in red. It ranked first, third, third, and third in terms of the four metrics respectively.

Since CASP16, PSBench has been substantially expanded by including the structural models of 2,002 new non-redundant targets deposited in the PDB between July 2024 and August 2025. We will continue to extend PSBench by incorporating structural models for more targets (e.g., the targets of the upcoming 2026 CASP17 competition and newly released protein complex structures in the PDB). Most models in PSBench were generated by AlphaFold, reflecting its current dominance but also introducing potential method-specific bias (see Appendix A.14 for detailed analysis). As new structure prediction methods emerge, we will incorporate their models into PSBench to further expand the diversity of prediction approaches represented in PSBench. We have also provided the model annotation pipeline in PSBench for third-party users to automatically label structural models generated in their research. New quality metrics that emerge in the field will be incorporated into PSBench to ensure the benchmark remains comprehensive and up to date. In addition, we benchmarked the runtime and memory usage of the baseline EMA methods (see Appendix B.7), which highlights the trade-off between the higher accuracy of multi-model EMA approaches such as GATE and the greater efficiency of lightweight single-model EMA methods. Finally, we provide a web server to accept structural models contributed by third-parties and will acknowledge their contribution in the future release of PSBench. Our goal is to make PSBench a community-driven resource like ImageNet or MNIST to support AI researchers to solve the critical protein model accuracy estimation problem.

7 Data and Software Availability

Data Availability

The PSBench datasets are publicly available at Harvard Dataverse: `https://dataverse.harvard.edu/dataset.xhtml?persistentId=doi:10.7910/DVN/75SZ1U`. DOI: `https://doi.org/10.7910/DVN/75SZ1U`.

Software Availability

The programs to evaluate EMA methods on the benchmark datasets, to generate labels for new datasets, and a web server for third-party model upload are available at GitHub: `https://github.com/BioinfoMachineLearning/PSBench`. The requirements to run PSBench are described in Appendix C.

8 Acknowledgment

We would like to thank the CASP organizers and community for sharing CASP15 and CASP16 data and NSF (award #: DBI2308699)) and NIH (award #: R01GM146340) for supporting this research.

References

[1] John Jumper, Richard Evans, Alexander Pritzel, Tim Green, Michael Figurnov, Olaf Ronneberger, Kathryn Tunyasuvunakool, Russ Bates, Augustin Žídek, Anna Potapenko, et al. Highly accurate protein structure prediction with alphafold. *nature*, 596(7873):583–589, 2021.

[2] Minkyung Baek, Frank DiMaio, Ivan Anishchenko, Justas Dauparas, Sergey Ovchinnikov, Gyu Rie Lee, Jue Wang, Qian Cong, Lisa N Kinch, R Dustin Schaeffer, et al. Accurate prediction of protein structures and interactions using a three-track neural network. *Science*, 373(6557):871–876, 2021.

[3] Jesse Eickholt and Jianlin Cheng. Predicting protein residue–residue contacts using deep networks and boosting. *Bioinformatics*, 28(23):3066–3072, 2012.

[4] Zhiye Guo, Tianqi Wu, Jian Liu, Jie Hou, and Jianlin Cheng. Improving deep learning-based protein distance prediction in casp14. *Bioinformatics*, 37(19):3190–3196, 2021.

[5] Jian Liu, Tianqi Wu, Zhiye Guo, Jie Hou, and Jianlin Cheng. Improving protein tertiary structure prediction by deep learning and distance prediction in casp14. *Proteins: Structure, Function, and Bioinformatics*, 90(1):58–72, 2022.

[6] Zhiye Guo, Jian Liu, Jeffrey Skolnick, and Jianlin Cheng. Prediction of inter-chain distance maps of protein complexes with 2d attention-based deep neural networks. *Nature Communications*, 13(1):6963, 2022.

[7] Jian Liu, Zhiye Guo, Tianqi Wu, Raj S Roy, Chen Chen, and Jianlin Cheng. Improving alphafold2-based protein tertiary structure prediction with multicom in casp15. *Communications chemistry*, 6(1):188, 2023.

[8] Jian Liu, Zhiye Guo, Tianqi Wu, Raj S Roy, Farhan Quadir, Chen Chen, and Jianlin Cheng. Enhancing alphafold-multimer-based protein complex structure prediction with multicom in casp15. *Communications biology*, 6(1):1140, 2023.

[9] Jian Liu, Pawan Neupane, and Jianlin Cheng. Improving AlphaFold2- and AlphaFold3-Based Protein Complex Structure Prediction With MULTICOM4 in CASP16. *Proteins: Structure, Function, and Bioinformatics*, 2025.

[10] Richard Evans, Michael O'Neill, Alexander Pritzel, Natasha Antropova, Andrew Senior, Tim Green, Augustin Žídek, Russ Bates, Sam Blackwell, Jason Yim, et al. Protein complex prediction with alphafold-multimer. *biorxiv*, pages 2021–10, 2021.

[11] Josh Abramson, Jonas Adler, Jack Dunger, Richard Evans, Tim Green, Alexander Pritzel, Olaf Ronneberger, Lindsay Willmore, Andrew J Ballard, Joshua Bambrick, et al. Accurate structure prediction of biomolecular interactions with alphafold 3. *Nature*, 630(8016):493–500, 2024.

[12] Chen Chen, Xiao Chen, Alex Morehead, Tianqi Wu, and Jianlin Cheng. 3d-equivariant graph neural networks for protein model quality assessment. *Bioinformatics*, 39(1):btad030, 2023.

[13] Andriy Kryshtafovych, Maciej Antczak, Marta Szachniuk, Tomasz Zok, Rachael C Kretsch, Ramya Rangan, Phillip Pham, Rhiju Das, Xavier Robin, Gabriel Studer, et al. New prediction categories in casp15. *Proteins: Structure, Function, and Bioinformatics*, 91(12):1550–1557, 2023.

[14] Andriy Kryshtafovych, Torsten Schwede, Maya Topf, Krzysztof Fidelis, and John Moult. Critical assessment of methods of protein structure prediction (casp)—round xv. *Proteins: Structure, Function, and Bioinformatics*, 91(12):1539–1549, 2023.

[15] Leila T Alexander, Janani Durairaj, Andriy Kryshtafovych, Luciano A Abriata, Yusupha Bayo, Gira Bhabha, Cécile Breyton, Simon G Caulton, James Chen, Séraphine Degroux, et al. Protein target highlights in casp15: Analysis of models by structure providers. *Proteins: Structure, Function, and Bioinformatics*, 91(12):1571–1599, 2023.

[16] Marc F Lensink, Guillaume Brysbaert, Nessim Raouraoua, Paul A Bates, Marco Giulini, Rodrigo V Honorato, Charlotte van Noort, Joao MC Teixeira, Alexandre MJJ Bonvin, Ren Kong, et al. Impact of alphafold on structure prediction of protein complexes: The casp15-capri experiment. *Proteins: Structure, Function, and Bioinformatics*, 91(12):1658–1683, 2023.

[17] Jing Zhang, Rongqing Yuan, Andriy Kryshtafovych, Rachael C Kretsch, R Dustin Schaeffer, Jian Zhou, Rhiju Das, Nick V Grishin, and Qian Cong. Assessment of protein complex predictions in casp16: Are we making progress? *bioRxiv*, pages 2025–05, 2025.

[18] Jian Liu, Pawan Neupane, and Jianlin Cheng. Estimating protein complex model accuracy using graph transformers and pairwise similarity graphs. *Bioinformatics Advances*, 5(1):vbaf180, 2025.

[19] Hongyi Zhou and Yaoqi Zhou. Distance-scaled, finite ideal-gas reference state improves structure-derived potentials of mean force for structure selection and stability prediction. *Protein science*, 11(11):2714–2726, 2002.

[20] Min-yi Shen and Andrej Sali. Statistical potential for assessment and prediction of protein structures. *Protein science*, 15(11):2507–2524, 2006.

[21] Renzhi Cao, Badri Adhikari, Debswapna Bhattacharya, Miao Sun, Jie Hou, and Jianlin Cheng. Qacon: single model quality assessment using protein structural and contact information with machine learning techniques. *Bioinformatics*, 33(4):586–588, 2017.

[22] Karolis Uziela and Björn Wallner. Proq2: estimation of model accuracy implemented in rosetta. *Bioinformatics*, 32(9):1411–1413, 2016.

[23] Cunliang Geng, Yong Jung, Nicolas Renaud, Vasant Honavar, Alexandre MJJ Bonvin, and Li C Xue. iscore: a novel graph kernel-based function for scoring protein–protein docking models. *Bioinformatics*, 36(1):112–121, 2020.

[24] Thom Vreven, Iain H Moal, Anna Vangone, Brian G Pierce, Panagiotis L Kastritis, Mieczyslaw Torchala, Raphael Chaleil, Brian Jiménez-García, Paul A Bates, Juan Fernandez-Recio, et al. Updates to the integrated protein–protein interaction benchmarks: docking benchmark version 5 and affinity benchmark version 2. *Journal of molecular biology*, 427(19):3031–3041, 2015.

[25] Jinchao Yu and Raphaël Guerois. Ppi4dock: large scale assessment of the use of homology models in free docking over more than 1000 realistic targets. *Bioinformatics*, 32(24):3760–3767, 2016.

[26] Ian Kotthoff, Petras J Kundrotas, and Ilya A Vakser. Dockground scoring benchmarks for protein docking. *Proteins: Structure, Function, and Bioinformatics*, 90(6):1259–1266, 2022.

[27] Mieczyslaw Torchala, Iain H Moal, Raphael AG Chaleil, Juan Fernandez-Recio, and Paul A Bates. Swarmdock: a server for flexible protein–protein docking. *Bioinformatics*, 29(6):807–809, 2013.

[28] Brian G Pierce, Kevin Wiehe, Howook Hwang, Bong-Hyun Kim, Thom Vreven, and Zhiping Weng. Zdock server: interactive docking prediction of protein–protein complexes and symmetric multimers. *Bioinformatics*, 30(12):1771–1773, 2014.

[29] Tammy Man-Kuang Cheng, Tom L Blundell, and Juan Fernandez-Recio. pydock: Electrostatics and desolvation for effective scoring of rigid-body protein–protein docking. *Proteins: Structure, Function, and Bioinformatics*, 68(2):503–515, 2007.

[30] Marc F Lensink and Shoshana J Wodak. Score_set: a capri benchmark for scoring protein complexes. *Proteins: Structure, Function, and Bioinformatics*, 82(11):3163–3169, 2014.

[31] Xiao Chen, Alex Morehead, Jian Liu, and Jianlin Cheng. A gated graph transformer for protein complex structure quality assessment and its performance in casp15. *Bioinformatics*, 39(Supplement_1):i308–i317, 2023.

[32] Lei Zhang, Sheng Wang, Jie Hou, Dong Si, Junyong Zhu, and Renzhi Cao. Complexqa: A deep graph learning approach for protein complex structure assessment. *Briefings in bioinformatics*, 24(6):bbad287, 2023.

[33] Marco Biasini, Tobias Schmidt, Stefan Bienert, Valerio Mariani, Gabriel Studer, Jürgen Haas, Niklaus Johner, Andreas Daniel Schenk, Ansgar Philippsen, and Torsten Schwede. Openstructure: an integrated software framework for computational structural biology. *Biological crystallography*, 69(5):701–709, 2013.

[34] Martino Bertoni, Florian Kiefer, Marco Biasini, Lorenza Bordoli, and Torsten Schwede. Modeling protein quaternary structure of homo-and hetero-oligomers beyond binary interactions by homology. *Scientific reports*, 7(1):10480, 2017.

[35] Valerio Mariani, Marco Biasini, Alessandro Barbato, and Torsten Schwede. lddt: a local superposition-free score for comparing protein structures and models using distance difference tests. *Bioinformatics*, 29(21):2722–2728, 2013.

[36] Chengxin Zhang, Morgan Shine, Anna Marie Pyle, and Yang Zhang. Us-align: universal structure alignments of proteins, nucleic acids, and macromolecular complexes. *Nature methods*, 19(9):1109–1115, 2022.

[37] Zeming Lin, Halil Akin, Roshan Rao, Brian Hie, Zhongkai Zhu, Wenting Lu, Nikita Smetanin, Allan dos Santos Costa, Maryam Fazel-Zarandi, Tom Sercu, Sal Candido, et al. Language models of protein sequences at the scale of evolution enable accurate structure prediction. *bioRxiv*, 2022.

[38] Kliment Olechnovič and Česlovas Venclovas. Voroif-gnn: Voronoi tessellation-derived protein–protein interface assessment using a graph neural network. *Proteins: Structure, Function, and Bioinformatics*, 91(12):1879–1888, 2023.

[39] Alex Morehead, Jian Liu, and Jianlin Cheng. Protein structure accuracy estimation using geometry-complete perceptron networks. *Protein Science*, 33(3):e4932, 2024.

[40] Raj S Roy, Jian Liu, Nabin Giri, Zhiye Guo, and Jianlin Cheng. Combining pairwise structural similarity and deep learning interface contact prediction to estimate protein complex model accuracy in casp15. *Proteins: Structure, Function, and Bioinformatics*, 91(12):1889–1902, 2023.

[41] Alisia Fadini, Recep Adiyaman, Shaima N Alhaddad, Behnosh Behzadi, Jianlin Cheng, Xinyue Cui, Nicholas S Edmunds, Lydia Freddolino, Ahmet G Genc, Fang Liang, et al. Highlights of model quality assessment in casp16. *Proteins: Structure, Function, and Bioinformatics*, 2025.

[42] Simon Mitternacht. Freesasa: An open source c library for solvent accessible surface area calculations. *F1000Research*, 5:189, 2016.

[43] Patrick Bryant, Gabriele Pozzati, Wensi Zhu, Aditi Shenoy, Petras Kundrotas, and Arne Elofsson. Predicting the structure of large protein complexes using alphafold and monte carlo tree search. *Nature communications*, 13(1):6028, 2022.

[44] Patrick Bryant, Gabriele Pozzati, and Arne Elofsson. Improved prediction of protein-protein interactions using alphafold2. *Nature communications*, 13(1):1265, 2022.

NeurIPS Paper Checklist

1. **Claims**

   Question: Do the main claims made in the abstract and introduction accurately reflect the paper's contributions and scope?

   Answer: [Yes]

   Justification: The abstract and introduction accurately reflect the paper's scope and contributions. They clearly motivate the need for robust Estimation of Model Accuracy (EMA) methods in protein complex structure prediction and identify the lack of large, diverse, and well-annotated datasets as a key barrier to develop them. The main claims include the introduction of PSBench, a benchmark suite comprising five large-scale datasets: four generated during CASP15 and CASP16, and one newly curated for new PDB entries deposited between July 2024 and August 2025. PSBench also provides extensive model quality annotations, standardized evaluation metrics, baseline EMA methods, and an automated evaluation pipeline. These claims are supported by the content of the paper and are appropriately scoped.

   Guidelines:

   - The answer NA means that the abstract and introduction do not include the claims made in the paper.
   - The abstract and/or introduction should clearly state the claims made, including the contributions made in the paper and important assumptions and limitations. A No or NA answer to this question will not be perceived well by the reviewers.
   - The claims made should match theoretical and experimental results, and reflect how much the results can be expected to generalize to other settings.
   - It is fine to include aspirational goals as motivation as long as it is clear that these goals are not attained by the paper.

2. **Limitations**

   Question: Does the paper discuss the limitations of the work performed by the authors?

   Answer: [Yes]

   Justification: The limitation regarding the potential bias in the protein structure prediction methods used to generate the datasets is discussed in Section 6. There is a future plan to address the limitation by incorporating structural models generated by new structure prediction methods. In addition, PSBench provides a web interface that allows third parties to contribute their own models to PSBench, ensuring that the benchmark remains comprehensive, diverse, and up to date.

   Guidelines:

   - The answer NA means that the paper has no limitation while the answer No means that the paper has limitations, but those are not discussed in the paper.
   - The authors are encouraged to create a separate "Limitations" section in their paper.
   - The paper should point out any strong assumptions and how robust the results are to violations of these assumptions (e.g., independence assumptions, noiseless settings, model well-specification, asymptotic approximations only holding locally). The authors should reflect on how these assumptions might be violated in practice and what the implications would be.
   - The authors should reflect on the scope of the claims made, e.g., if the approach was only tested on a few datasets or with a few runs. In general, empirical results often depend on implicit assumptions, which should be articulated.
   - The authors should reflect on the factors that influence the performance of the approach. For example, a facial recognition algorithm may perform poorly when image resolution is low or images are taken in low lighting. Or a speech-to-text system might not be used reliably to provide closed captions for online lectures because it fails to handle technical jargon.
   - The authors should discuss the computational efficiency of the proposed algorithms and how they scale with dataset size.

- If applicable, the authors should discuss possible limitations of their approach to address problems of privacy and fairness.
- While the authors might fear that complete honesty about limitations might be used by reviewers as grounds for rejection, a worse outcome might be that reviewers discover limitations that aren't acknowledged in the paper. The authors should use their best judgment and recognize that individual actions in favor of transparency play an important role in developing norms that preserve the integrity of the community. Reviewers will be specifically instructed to not penalize honesty concerning limitations.

3. **Theory assumptions and proofs**

   Question: For each theoretical result, does the paper provide the full set of assumptions and a complete (and correct) proof?

   Answer: [NA]

   Justification: We only include practical/experimental results.

   Guidelines:

   - The answer NA means that the paper does not include theoretical results.
   - All the theorems, formulas, and proofs in the paper should be numbered and cross-referenced.
   - All assumptions should be clearly stated or referenced in the statement of any theorems.
   - The proofs can either appear in the main paper or the supplemental material, but if they appear in the supplemental material, the authors are encouraged to provide a short proof sketch to provide intuition.
   - Inversely, any informal proof provided in the core of the paper should be complemented by formal proofs provided in appendix or supplemental material.
   - Theorems and Lemmas that the proof relies upon should be properly referenced.

4. **Experimental result reproducibility**

   Question: Does the paper fully disclose all the information needed to reproduce the main experimental results of the paper to the extent that it affects the main claims and/or conclusions of the paper (regardless of whether the code and data are provided or not)?

   Answer: [Yes]

   Justification: The paper provides comprehensive details necessary to reproduce the main experimental results. This includes detailed procedures for generating model quality scores using the annotation pipeline described in Appendix A.3 (Preprocessing, Implementation Details, and Edge Cases of the Annotation Pipeline), as well as descriptions of the experimental setup, training and validation protocols, evaluation metrics, and baseline EMA methods presented in Sections 4, 5, and Appendix B. The datasets are hosted on Harvard Dataverse (`https://doi.org/10.7910/DVN/75SZ1U`) and the source codes of the structural model quality annotations and evaluation are available on GitHub (`https://github.com/BioinfoMachineLearning/PSBench`), as noted in Section 7. Detailed reproduction instructions are provided in the GitHub repository under the section *III. Reproducing the evaluation results of GATE and other baseline EMA methods in PSBench*, ensuring that other researchers can replicate and verify the findings.

   Guidelines:

   - The answer NA means that the paper does not include experiments.
   - If the paper includes experiments, a No answer to this question will not be perceived well by the reviewers: Making the paper reproducible is important, regardless of whether the code and data are provided or not.
   - If the contribution is a dataset and/or model, the authors should describe the steps taken to make their results reproducible or verifiable.
   - Depending on the contribution, reproducibility can be accomplished in various ways. For example, if the contribution is a novel architecture, describing the architecture fully might suffice, or if the contribution is a specific model and empirical evaluation, it may be necessary to either make it possible for others to replicate the model with the same dataset, or provide access to the model. In general. releasing code and data is often

one good way to accomplish this, but reproducibility can also be provided via detailed instructions for how to replicate the results, access to a hosted model (e.g., in the case of a large language model), releasing of a model checkpoint, or other means that are appropriate to the research performed.

- While NeurIPS does not require releasing code, the conference does require all submissions to provide some reasonable avenue for reproducibility, which may depend on the nature of the contribution. For example
  (a) If the contribution is primarily a new algorithm, the paper should make it clear how to reproduce that algorithm.
  (b) If the contribution is primarily a new model architecture, the paper should describe the architecture clearly and fully.
  (c) If the contribution is a new model (e.g., a large language model), then there should either be a way to access this model for reproducing the results or a way to reproduce the model (e.g., with an open-source dataset or instructions for how to construct the dataset).
  (d) We recognize that reproducibility may be tricky in some cases, in which case authors are welcome to describe the particular way they provide for reproducibility. In the case of closed-source models, it may be that access to the model is limited in some way (e.g., to registered users), but it should be possible for other researchers to have some path to reproducing or verifying the results.

5. **Open access to data and code**

Question: Does the paper provide open access to the data and code, with sufficient instructions to faithfully reproduce the main experimental results, as described in supplemental material?

Answer: [Yes]

Justification: The open source data are released at Harvard Dataverse with DOI: `https://doi.org/10.7910/DVN/75SZ1U` and the source code is available on GitHub: `https://github.com/BioinfoMachineLearning/PSBench`, as described in Section 7. Detailed instructions for reproducing the EMA evaluation results using PSBench in Section 5 are provided in the GitHub repository under the section *III. Reproducing the evaluation results of GATE and other baseline EMA methods in PSBench*.

Guidelines:

- The answer NA means that paper does not include experiments requiring code.
- Please see the NeurIPS code and data submission guidelines (`https://nips.cc/public/guides/CodeSubmissionPolicy`) for more details.
- While we encourage the release of code and data, we understand that this might not be possible, so “No” is an acceptable answer. Papers cannot be rejected simply for not including code, unless this is central to the contribution (e.g., for a new open-source benchmark).
- The instructions should contain the exact command and environment needed to run to reproduce the results. See the NeurIPS code and data submission guidelines (`https://nips.cc/public/guides/CodeSubmissionPolicy`) for more details.
- The authors should provide instructions on data access and preparation, including how to access the raw data, preprocessed data, intermediate data, and generated data, etc.
- The authors should provide scripts to reproduce all experimental results for the new proposed method and baselines. If only a subset of experiments are reproducible, they should state which ones are omitted from the script and why.
- At submission time, to preserve anonymity, the authors should release anonymized versions (if applicable).
- Providing as much information as possible in supplemental material (appended to the paper) is recommended, but including URLs to data and code is permitted.

6. **Experimental setting/details**

Question: Does the paper specify all the training and test details (e.g., data splits, hyperparameters, how they were chosen, type of optimizer, etc.) necessary to understand the results?

Answer: [Yes]

Justification: We provide the training, validation and test details of GATE/GATE-AFM in Section 4.2 and Appendix B.2.

Guidelines:

- The answer NA means that the paper does not include experiments.
- The experimental setting should be presented in the core of the paper to a level of detail that is necessary to appreciate the results and make sense of them.
- The full details can be provided either with the code, in appendix, or as supplemental material.

7. **Experiment statistical significance**

Question: Does the paper report error bars suitably and correctly defined or other appropriate information about the statistical significance of the experiments?

Answer: [Yes]

Justification: We have performed statistical significance test between GATE-AFM and other EMA methods for the results shown in Table 1, as described in Section 5.1. Statistically significant differences were determined using the one-sided Wilcoxon signed-rank test and are annotated in the table with appropriate symbols.

Guidelines:

- The answer NA means that the paper does not include experiments.
- The authors should answer "Yes" if the results are accompanied by error bars, confidence intervals, or statistical significance tests, at least for the experiments that support the main claims of the paper.
- The factors of variability that the error bars are capturing should be clearly stated (for example, train/test split, initialization, random drawing of some parameter, or overall run with given experimental conditions).
- The method for calculating the error bars should be explained (closed form formula, call to a library function, bootstrap, etc.)
- The assumptions made should be given (e.g., Normally distributed errors).
- It should be clear whether the error bar is the standard deviation or the standard error of the mean.
- It is OK to report 1-sigma error bars, but one should state it. The authors should preferably report a 2-sigma error bar than state that they have a 96% CI, if the hypothesis of Normality of errors is not verified.
- For asymmetric distributions, the authors should be careful not to show in tables or figures symmetric error bars that would yield results that are out of range (e.g. negative error rates).
- If error bars are reported in tables or plots, The authors should explain in the text how they were calculated and reference the corresponding figures or tables in the text.

8. **Experiments compute resources**

Question: For each experiment, does the paper provide sufficient information on the computer resources (type of compute workers, memory, time of execution) needed to reproduce the experiments?

Answer: [Yes]

Justification: This paper presents the system requirements in Appendix C.

Guidelines:

- The answer NA means that the paper does not include experiments.
- The paper should indicate the type of compute workers CPU or GPU, internal cluster, or cloud provider, including relevant memory and storage.
- The paper should provide the amount of compute required for each of the individual experimental runs as well as estimate the total compute.

- The paper should disclose whether the full research project required more compute than the experiments reported in the paper (e.g., preliminary or failed experiments that didn't make it into the paper).

9. **Code of ethics**

   Question: Does the research conducted in the paper conform, in every respect, with the NeurIPS Code of Ethics `https://neurips.cc/public/EthicsGuidelines`?

   Answer: [Yes]

   Justification: The research conducted fully complies with the NeurIPS Code of Ethics.

   Guidelines:

   - The answer NA means that the authors have not reviewed the NeurIPS Code of Ethics.
   - If the authors answer No, they should explain the special circumstances that require a deviation from the Code of Ethics.
   - The authors should make sure to preserve anonymity (e.g., if there is a special consideration due to laws or regulations in their jurisdiction).

10. **Broader impacts**

    Question: Does the paper discuss both potential positive societal impacts and negative societal impacts of the work performed?

    Answer: [Yes]

    Justification: The paper discusses potential societal impacts. On the positive side, PSBench enables the development of more accurate and reliable EMA methods, which can improve downstream applications in protein function annotation, drug discovery, and disease understanding. These advances could accelerate biomedical research and therapeutic development. No negative impact is noticed.

    Guidelines:

    - The answer NA means that there is no societal impact of the work performed.
    - If the authors answer NA or No, they should explain why their work has no societal impact or why the paper does not address societal impact.
    - Examples of negative societal impacts include potential malicious or unintended uses (e.g., disinformation, generating fake profiles, surveillance), fairness considerations (e.g., deployment of technologies that could make decisions that unfairly impact specific groups), privacy considerations, and security considerations.
    - The conference expects that many papers will be foundational research and not tied to particular applications, let alone deployments. However, if there is a direct path to any negative applications, the authors should point it out. For example, it is legitimate to point out that an improvement in the quality of generative models could be used to generate deepfakes for disinformation. On the other hand, it is not needed to point out that a generic algorithm for optimizing neural networks could enable people to train models that generate Deepfakes faster.
    - The authors should consider possible harms that could arise when the technology is being used as intended and functioning correctly, harms that could arise when the technology is being used as intended but gives incorrect results, and harms following from (intentional or unintentional) misuse of the technology.
    - If there are negative societal impacts, the authors could also discuss possible mitigation strategies (e.g., gated release of models, providing defenses in addition to attacks, mechanisms for monitoring misuse, mechanisms to monitor how a system learns from feedback over time, improving the efficiency and accessibility of ML).

11. **Safeguards**

    Question: Does the paper describe safeguards that have been put in place for responsible release of data or models that have a high risk for misuse (e.g., pretrained language models, image generators, or scraped datasets)?

    Answer: [NA]

    Justification: This paper poses no such risks.

Guidelines:

- The answer NA means that the paper poses no such risks.
- Released models that have a high risk for misuse or dual-use should be released with necessary safeguards to allow for controlled use of the model, for example by requiring that users adhere to usage guidelines or restrictions to access the model or implementing safety filters.
- Datasets that have been scraped from the Internet could pose safety risks. The authors should describe how they avoided releasing unsafe images.
- We recognize that providing effective safeguards is challenging, and many papers do not require this, but we encourage authors to take this into account and make a best faith effort.

12. **Licenses for existing assets**

Question: Are the creators or original owners of assets (e.g., code, data, models), used in the paper, properly credited and are the license and terms of use explicitly mentioned and properly respected?

Answer: [Yes]

Justification: All tools and external datasets used in this work have been appropriately cited in the paper and acknowledged within the GitHub repository. The source code is released under the MIT License, and the dataset is made available on Harvard Dataverse under the CC0 1.0 Public Domain Dedication, permitting unrestricted use, distribution, and reproduction in any medium without limitation.

Guidelines:

- The answer NA means that the paper does not use existing assets.
- The authors should cite the original paper that produced the code package or dataset.
- The authors should state which version of the asset is used and, if possible, include a URL.
- The name of the license (e.g., CC-BY 4.0) should be included for each asset.
- For scraped data from a particular source (e.g., website), the copyright and terms of service of that source should be provided.
- If assets are released, the license, copyright information, and terms of use in the package should be provided. For popular datasets, `paperswithcode.com/datasets` has curated licenses for some datasets. Their licensing guide can help determine the license of a dataset.
- For existing datasets that are re-packaged, both the original license and the license of the derived asset (if it has changed) should be provided.
- If this information is not available online, the authors are encouraged to reach out to the asset's creators.

13. **New assets**

Question: Are new assets introduced in the paper well documented and is the documentation provided alongside the assets?

Answer: [Yes]

Justification: This paper introduces datasets and tools, which are thoroughly documented in the paper, the GitHub repository, and the Harvard Dataverse. Documentation includes dataset descriptions, usage instructions, licensing information, and relevant limitations. No human subjects were involved, so consent was not required.

Guidelines:

- The answer NA means that the paper does not release new assets.
- Researchers should communicate the details of the dataset/code/model as part of their submissions via structured templates. This includes details about training, license, limitations, etc.
- The paper should discuss whether and how consent was obtained from people whose asset is used.

- At submission time, remember to anonymize your assets (if applicable). You can either create an anonymized URL or include an anonymized zip file.

14. **Crowdsourcing and research with human subjects**

    Question: For crowdsourcing experiments and research with human subjects, does the paper include the full text of instructions given to participants and screenshots, if applicable, as well as details about compensation (if any)?

    Answer: [NA]

    Justification: We do not involve crowdsourcing or research with human subjects.

    Guidelines:

    - The answer NA means that the paper does not involve crowdsourcing nor research with human subjects.
    - Including this information in the supplemental material is fine, but if the main contribution of the paper involves human subjects, then as much detail as possible should be included in the main paper.
    - According to the NeurIPS Code of Ethics, workers involved in data collection, curation, or other labor should be paid at least the minimum wage in the country of the data collector.

15. **Institutional review board (IRB) approvals or equivalent for research with human subjects**

    Question: Does the paper describe potential risks incurred by study participants, whether such risks were disclosed to the subjects, and whether Institutional Review Board (IRB) approvals (or an equivalent approval/review based on the requirements of your country or institution) were obtained?

    Answer: [NA]

    Justification: We do not involve crowdsourcing or research with human subjects.

    Guidelines:

    - The answer NA means that the paper does not involve crowdsourcing nor research with human subjects.
    - Depending on the country in which research is conducted, IRB approval (or equivalent) may be required for any human subjects research. If you obtained IRB approval, you should clearly state this in the paper.
    - We recognize that the procedures for this may vary significantly between institutions and locations, and we expect authors to adhere to the NeurIPS Code of Ethics and the guidelines for their institution.
    - For initial submissions, do not include any information that would break anonymity (if applicable), such as the institution conducting the review.

16. **Declaration of LLM usage**

    Question: Does the paper describe the usage of LLMs if it is an important, original, or non-standard component of the core methods in this research? Note that if the LLM is used only for writing, editing, or formatting purposes and does not impact the core methodology, scientific rigorousness, or originality of the research, declaration is not required.

    Answer: [NA]

    Justification: LLM is not directly involved as any important, original, or non-standard component in this study.

    Guidelines:

    - The answer NA means that the core method development in this research does not involve LLMs as any important, original, or non-standard components.
    - Please refer to our LLM policy (`https://neurips.cc/Conferences/2025/LLM`) for what should or should not be described.

A Dataset Design

A.1 Diversity of Protein Complex Targets in PSBench

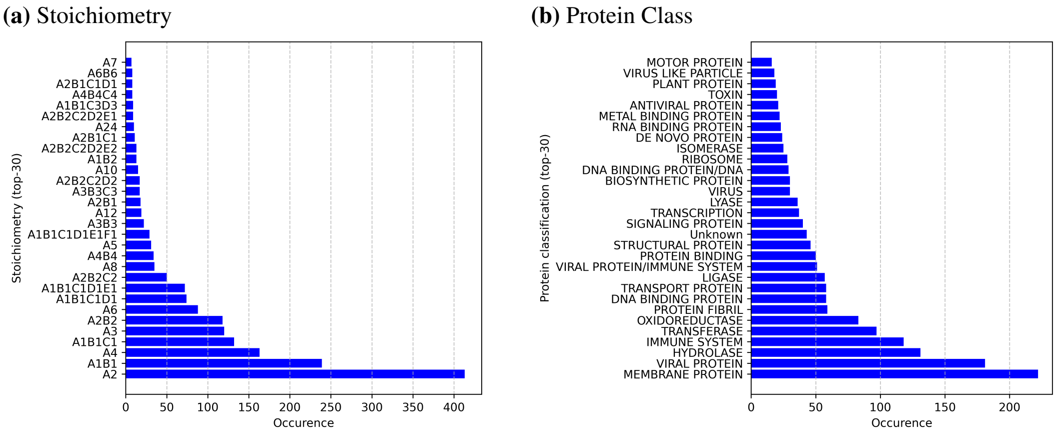
(a) Stoichiometry

(b) Protein Class

Figure S1: Diversity of 2081 protein complex targets. (a) Number of targets for each of top-30 stoichiometries (out of 185) represented in PSBench. A stoichiometry is denoted by letters interleaved with numbers. Each letter represents a unique chain. The number following a letter is the number of the copies (count) of the chain. For instance, A1B2 means a complex has two unique chains A and B, while A has one copy and B has two copies. **(b)** Number of targets for each of top-30 broad protein function classes (out of 145) and an "Unknown" class in PSBench. "Unknown" means there is no class information and therefore may include many different classes.

A.2 Definitions of Quality Scores

PSBench provides a comprehensive list of quality scores for each protein complex structural model as labels, which are described below.

Global quality scores

- **tmscore** : The Template Modeling score (TM-score) measures structural similarity between a predicted structure and a reference structure, with higher values (above 0.8) indicating strong agreement. In our evaluation, four variants of the TM-score are used: **(1)** `tmscore_mmalign`, computed using OpenStructure with the USalign plugin and parameters `-mm 1 -ter 0`, following the CASP16 evaluation protocol; **(2)** `tmscore_usalign`, calculated with the USalign program using parameters `-ter 1 -TMscore 6`, aligning with the CASP15 evaluation protocol; **(3)** `tmscore_usalign_aligned`, which further incorporates residue-residue correspondence via an in-house alignment and filtration script before applying USalign with the same parameters; and **(4)** `tmscore_usalign_aligned_v0`, an earlier version based on a prior alignment script, used for generating GATE EMA training labels and available only for the CASP15_inhouse_dataset. Despite slight procedural differences, all variants apply a consistent threshold interpretation for assessing structural similarity.
- **rmsd** : The Root Mean Square Deviation (`rmsd`) measures the average distance between corresponding atoms in the model and target structures. It quantifies how much the predicted model deviates from the native structure, with lower values indicating a more accurate structure.

Local quality score

- **lddt** : The measures the agreement between inter-atomic distances in the model and the target structure. It evaluates how accurately the overall atomic arrangement is reproduced, focusing on all residues from all chains.

Interface quality scores

- **ics** : The Interface Contact Score(`ics`) measures how accurately predicted residue contacts between protein chains match the true contacts in the target structure. It is a weighted average of F1-scores for each chain-chain interface, where interfaces with more true contacts contribute more to the overall score.
- **ics_precision** : The Interface Contact Precision(`ics_precision`) measures how many predicted residue contacts are correct, focusing on prediction accuracy rather than coverage. It is a weighted average of precision for each chain-chain interface, with larger interfaces (more true contacts) contributing more to the final score.
- **ics_recall** : The Interface Contact Recall(`ics_recall`)measures how many true residue contacts are correctly predicted, focusing on coverage. It is a weighted average of recall for each chain-chain interface, with larger interfaces (more true contacts) contributing more to the final score.
- **ips** : The Interface Patch Similarity(`ips`) measures the similarity between predicted and true interface residue contacts using the Jaccard coefficient. It is a weighted average of the Jaccard index for each chain-chain interface, with larger interfaces (more true contacts) contributing more to the final score.
- **qs_global** : The QS (global) score(`qs_global`) measures the fraction of correctly predicted interface contacts relative to the total number of true or predicted contacts, whichever is larger. It reflects the overall accuracy of contact prediction across the entire protein complex.
- **qs_best** : The QS (best) score(`qs_best`) measures the highest fraction of correctly predicted interface contacts for any single chain-chain interface in the complex. It highlights the best-performing interface prediction within the entire structure.
- **dockq_wave** : The DockQ_wave(`dockq_wave`) measures the weighted average of DockQ scores across all chain-chain interfaces in the complex. It provides an overall measure of interface prediction quality, combining precision, recall, and Fnat into a single score.

A.3 Preprocessing, Implementation Details, and Edge Cases of the Annotation Pipeline

To enable fair and reproducible benchmarking of EMA methods, PSBench employs an automated annotation pipeline to compute quality scores for structural models using their corresponding native structures as references. This pipeline ensures that models from diverse sources are consistently aligned, compared, and labeled with multiple complementary accuracy measures.

Preprocessing. All native PDB structures were reindexed to match the full-length protein sequences. Non-protein components (e.g., ligands and metal ions) were excluded. If there are insertion codes (e.g., 85A, 86B) in the residue indices of the native structure, they are replaced with indices that correspond to the residue positions in the FASTA sequence. All subsequent residues are renumbered to ensure continuous, monotonic indexing without gaps or duplicates.

Alignment and quality score computation. After preprocessing, the pipeline aligns predicted and native structures based on sequence identity and computes scores such as RMSD and lDDT without requiring additional preprocessing. During alignment/evaluation, residues that are missing in the native PDB structure are automatically excluded by OpenStructure, so scoring is restricted to experimentally resolved regions. For TM-score, two routes were used: (i) `tmscore_mmalign`, via OpenStructure's embedded MM-align interface with CASP16-style parameters; and (ii) `tmscore_usalign`, via the standalone US-align program with CASP15-style parameters. For `tmscore_usalign_aligned`, we additionally applied a residue reindexing/filtration step to enforce residue–residue correspondence before running US-align; no such preprocessing was applied to `tmscore_usalign`. TM-score was interpreted following standard practice.

Edge cases. Despite the robustness of the pipeline, a small fraction of structural models from the CASP community datasets failed annotation due to format inconsistencies or violations of

OpenStructure's assumptions. For example, non-monotonic residue numbering (e.g., H1272TS191_1 from the `CASP16_community_dataset`) caused alignment failures, while malformed PDB files with duplicate atom labels (e.g., H1114TS229_1 from the `CASP15_community_dataset`) triggered parsing errors. When the number of valid residues in a chain is less than six, OpenStructure refuses to include such chains in chain mapping and evaluation.

Fallbacks and exclusions. When OpenStructure failed but US-align succeeded, we retained the model and reported the TM-score from US-align. For example, in the `Multimer_7_2024_8_2025_dataset`, OpenStructure fails for three targets (9DYY, 9KAP, and 9O7J) because all chains contain fewer than six valid residues. For these cases, only TM-scores computed using US-align are included. Models that failed under both frameworks were excluded. For our datasets, such failures were extremely rare, affecting fewer than 0.002% out of more than 1.4 million models.

Finally, it is worth noting that the native structures used as ground truth in PSBench, although experimentally determined, are not error-free. Some structures solved by X-ray crystallography, cryo-EM, or NMR may have some problems such as highly flexible regions, crystal artifacts, or low-resolution density. To mitigate these effects, PSBench limits the evaluation to resolved regions and incorporates local metrics (e.g., lDDT) that are less sensitive to global alignment noise. Users should therefore interpret benchmark results as reflecting both prediction accuracy and the inherent uncertainty of the experimental references.

A.4 Metric Redundancy Analysis

PSBench provides ten complementary quality metrics that capture different aspects of model accuracy, including global fold, residue-level details, and interfacial quality. While this diversity allows for more comprehensive evaluation, some metrics may be redundant due to overlapping definitions. To better understand their relationships, we analyzed metric redundancy across all five datasets.

The pairwise Pearson's correlation analysis (Figure S2a) indicates moderate to strong dependencies among several metrics. Among the interface contact–based measures, `ics` and `ics_precision` were strongly correlated ($r = 0.88$), and `ics` also showed substantial association with `ics_recall` ($r = 0.74$), indicating that these metrics capture overlapping aspects of interface accuracy. Similarly, `qs_best` and `qs_global` were closely related ($r = 0.76$), consistent with their shared focus on interface quality. `dockq_wave`, which integrates multiple interface-level components such as interface contact accuracy and interface RMSD into a single continuous score, showed moderate correlations with both interface-based metrics (`ics`: $r = 0.64$; `ics_recall`: $r = 0.72$) and global fold metrics (`tmscore_mmalign`: $r = 0.55$). This indicates that `dockq_wave` captures aspects of both local interface geometry and overall model correctness. In contrast, metrics that assess overall or local residue-level accuracy showed weaker correlations with interface-based measures. For example, `lddt` exhibited only moderate correlations with global and interface metrics ($r = 0.56$ with `dockq_wave`; $r = 0.47$ with `tmscore_mmalign`), reflecting its distinct sensitivity to local residue details. `tmscore_mmalign` and `rmsd` also showed moderate inter-metric correlations ($r \approx$ 0.3–0.7), suggesting complementary perspectives on overall structural similarity.

Principal Component Analysis (PCA) provided further insights into metric relationships as shown in Figure S2b. PC1 exhibited similar negative loadings across nearly all metrics (approximately –0.3), except for `rmsd`, which showed an opposite loading (0.20). This pattern indicates that PC1 captures a general dimension of overall model quality, where improvements in most metrics correspond to lower RMSD values. PC2 was primarily driven by `rmsd` (loading = 0.75), while PC3 was dominated by `lddt` (loading = 0.91). PC4 showed strong contributions from `tmscore_mmalign` (loading = 0.67) and `rmsd` (loading = 0.43). PC5 was characterized by `ips` (loading = 0.64) and `dockq_wave` (loading = -0.57). The variance information (Fig. S2c) shows that PC1 captures the vast majority of variance, with subsequent components contributing progressively less.

To account for redundancy when combining metrics during training, we propose a correlation-based weighting scheme. Each metric is weighted inversely to its average Pearson's correlation with the other metrics, i.e.,

$$w_i = \frac{1}{\frac{1}{N-1}\sum_{j\neq i} r_{ij}},$$

where r_{ij} is the correlation between metrics i and j, and N is the total number of metrics. This down-weights highly redundant metrics (e.g., ics, ics_precision, ics_recall) while giving more influence to complementary metrics such as lddt and ips.

The resulting weights can be applied in a weighted loss function to train EMA methods:

$$L(m) = \sum_{i=1}^{N} w_i \, \ell\big(\hat{y}_i(m), y_i(m)\big),$$

where $\ell(\cdot)$ is the loss (e.g., mean squared error) between the predicted score $\hat{y}_i(m)$ and the reference score $y_i(m)$ for metric i.

In practice, this means that highly correlated interface metrics contribute less to the final loss, while distinct signals such as those from lddt or rmsd are emphasized. This weighting ensures that training focuses on complementary information rather than duplicating signal from redundant metrics.

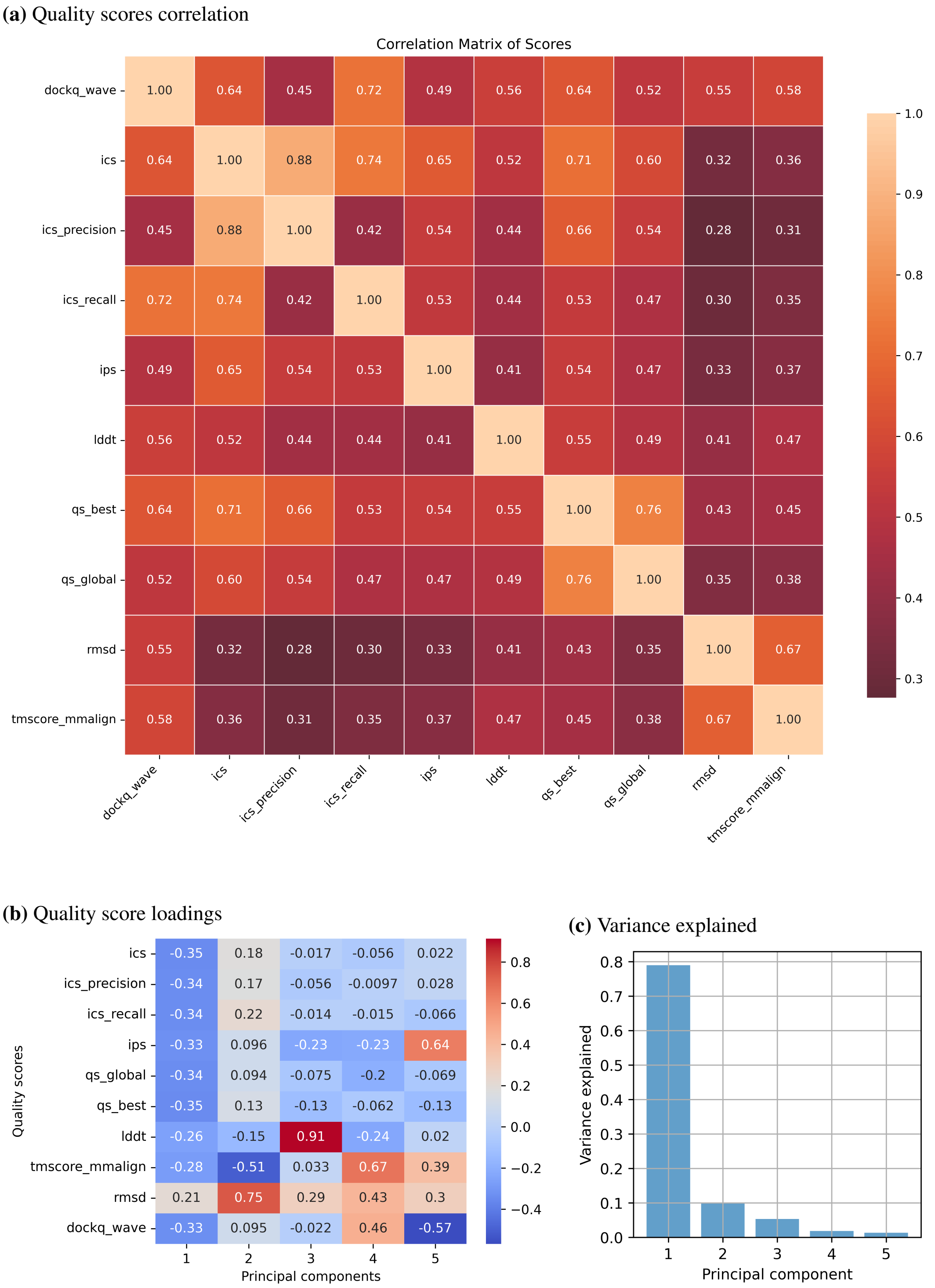
(a) Quality scores correlation

(b) Quality score loadings

(c) Variance explained

Figure S2: Relationships among quality scores. (a) Quality scores correlation. Pairwise correlation between different quality scores. **(b) Quality score loadings.** Loadings of each quality score on the first five principal components. **(c) Variance explained.** Variance explained by each principal component.

A.5 Relationship between interface contact density and interface quality scores

To assess how protein–protein interface contact density influences the stability of interface quality scores, we computed the variance of ICS, IPS, and QS_Best across the CASP15 and CASP16 community models for each target and examined their correlation with the native interface contact density. These datasets were selected because they consist of models from diverse sources for each target, reflecting the inherent variability in predicting structural models for a protein complex. Interface contact density was calculated as the ratio of residue-residue contacts to buried surface area (BSA). Residue pairs were considered in contact if any atoms were within 5.0 Å. BSA was computed using FreeSASA[42] with standard parameters as BSA(A,B) = SASA(chain A) + SASA(chain B) − SASA(A-B complex) for each chain pair, where SASA(chain) denotes the solvent-accessible surface area of the isolated chain, and SASA(A–B complex) represents that of the assembled complex. This difference quantifies the surface area that becomes inaccessible to solvent upon binding, corresponding to the interface area buried between the two chains. The mean contact density across all chain pairs is then used to compute the correlation with the variance of interface scores.

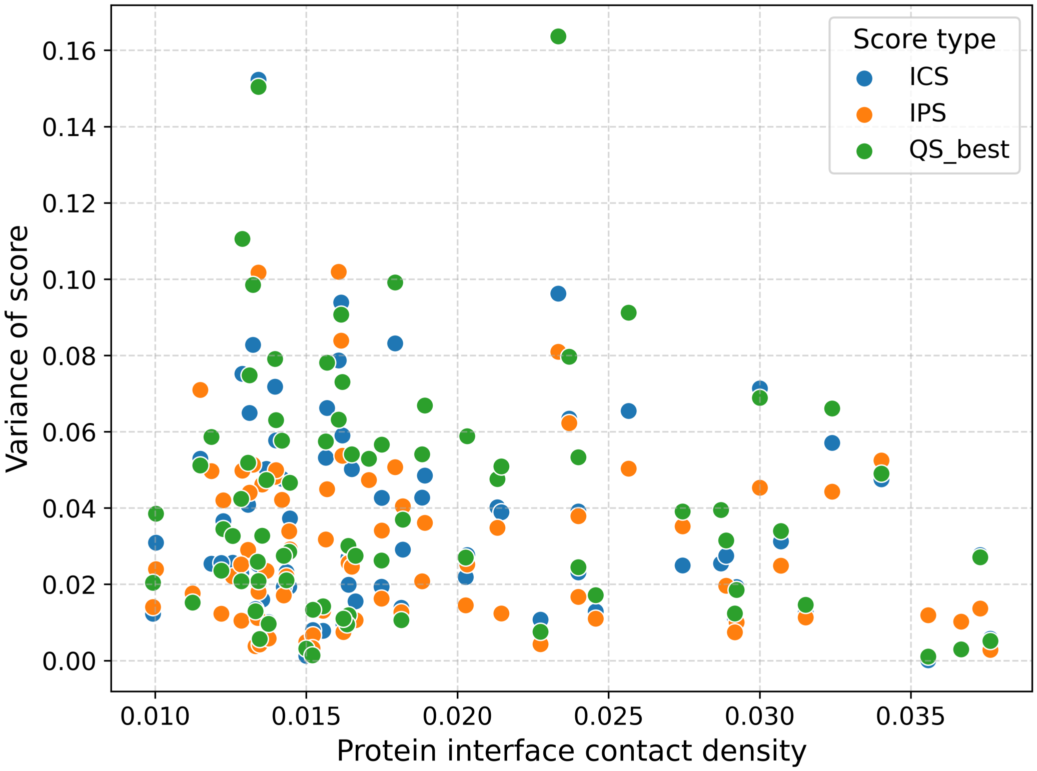

Figure S3: Variance of interface quality scores (`ICS`, `IPS`, `QS_best`) plotted against protein interface contact density. Weak negative correlations are observed for all three metrics (r=-0.125 for `ICS`, r=-0.126 for `IPS`, and r=-0.115 for `QS_best`), indicating little influence of contact density on score variability.

The relationship between interface contact density and the variance in interface quality scores was examined (Fig. S3). All three metrics—`ICS`, `IPS`, and `QS_Best`—showed weak negative correlations with contact density, with correlation coefficients of $r = -0.125$ for `ICS`, $r = -0.126$ for `IPS`, and $r = -0.115$ for `QS_Best`. The results indicate a weak inverse relationship between interface contact density and interface score variability, suggesting that while contact density does have some influence on the variability of these interface quality scores, its effect is relatively modest.

A.6 Guidance on Applications of Quality Scores

Global quality scores. TM-score variants (`tmscore`) are ideal for evaluating global fold accuracy in tasks such as structure-based function annotation and complex template retrieval, as they capture overall topology and are widely used in fold recognition benchmarks. RMSD is appropriate for atomic-level accuracy in applications such as structural refinement or drug binding site validation, where small positional deviations can impact function.

Local quality scores. Local Distance Difference Test (`lddt`) evaluates the accuracy of individual residue positions relative to their local environment, making it useful for residue-level analyses such as identifying flexible regions, validating side-chain placements, or assessing the accuracy of binding pocket geometry.

Interface quality scores. For interface-focused tasks such as docking, binder design, and epitope mapping, DockQ_Wave (`dockq_wave`) and Interface Patch Similarity (`ips`) provide comprehensive assessments of contact and interface quality. Interface Contact Precision (`ics_precision`) and Interface Contact Recall (`ics_recall`) evaluate the specificity and coverage of predicted contacts. The QS (global) score (`qs_global`) measures overall interface accuracy, while the QS (best) score (`qs_best`) highlights the highest-quality interface, which is particularly useful in asymmetric or functionally focused assemblies.

A.7 Additional Input Features for Structural Models in CASP15_inhouse_dataset and CASP16_inhouse_dataset

Each structural model in the four datasets in PSBench is stored as a PDB file, which contains the (x, y, z) coordinates of every atom in the model. In addition, the two in-house datasets (CASP15_inhouse_dataset and CASP16_inhouse_dataset) and their subsets include the following extra features for each structural model, which can be leveraged by EMA methods.

- **model_type** : The type determines whether the model is generated using AlphaFold2 or AlphaFold3. AlphaFold3-based models are only available for CASP16_inhouse_dataset and its subset.
- **afm_confidence_score** : The AlphaFold2-Multimer Confidence score (`afm_confidence_score`) determines the confidence score in multimeric protein structures primarily assessed using ipTM and pTM score. For AlphaFold2 program, the AFM confidence score is available upon the completition of the prediction, but for AlphaFold3-based models, since the AFM confidence score is not readily available, it is obtained by the calculation $0.8 \times iptm + 0.2 \times ptm$.
- **af3_ranking_score** : The AlphaFold3 Ranking score (`af3_ranking_score`) determines the ranking score as provided by AlphaFold3 program. It is only available for AlphaFold3 generated models in CASP16_inhouse_dataset.
- **iptm** : The Interface Predicted Template Modeling score(`ipTM`) evaluates the accuracy of the predicted relative positioning of subunits within a protein-protein complex. Scores above 0.8 indicate confident, high-quality predictions, while scores below 0.6 typically reflect failed predictions. Values between 0.6 and 0.8 fall into an intermediate range, where prediction quality is uncertain and may vary.
- **num_inter_pae** : Number of inter-chain predicted aligned errors (<5 Å).
- **mpDockQ[43]/pDockQ[44]** : Multiple-interface predicted DockQ for multimer, or predicted DockQ (pDockQ) for dimer.

A.8 CASP15_inhouse_dataset

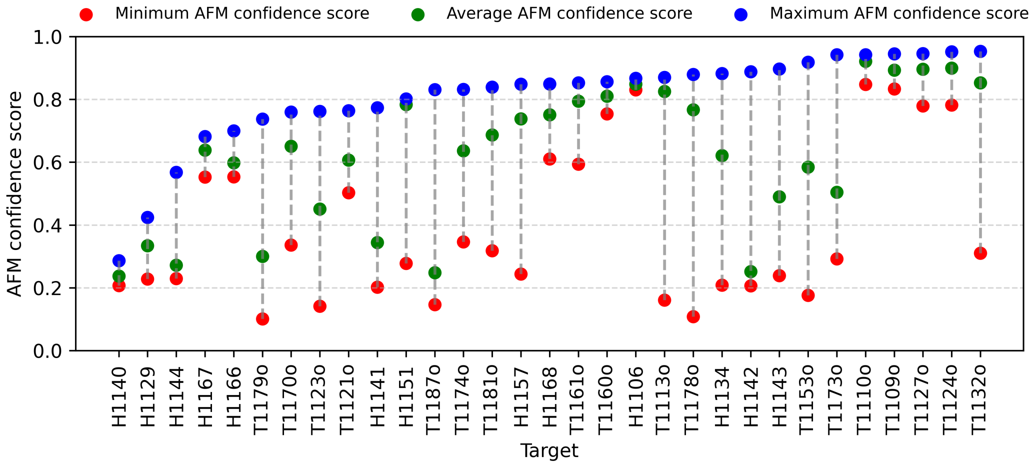

Figure S4: Distribution of AFM confidence scores per target in CASP15_inhouse_dataset.

Table S1: Summary of target information and number of models per target in CASP15_inhouse_dataset. It is worth noting that nine CASP15 targets (H1111, H1114, H1135, H1137, H1171, H1172, H1185, T1176o and T1192o) were excluded because they required alternative structure prediction approaches, such as template-based modeling, due to their large size or the limited number of the predicted structures (e.g., less than 30).

Target	Stoichiometry	Protein Classification	Seq. Length	Total models
H1106	A1B1	CHAPERONE	236	580
H1129	A1B1	MEMBRANE PROTEIN	1387	145
H1134	A1B1	TOXIN/IMMUNE SYSTEM	543	295
H1140	A1B1	PROTEIN BINDING	351	270
H1141	A1B1	PROTEIN BINDING	346	260
H1142	A1B1	PROTEIN BINDING	347	275
H1143	A1B1	PROTEIN BINDING	350	245
H1144	A1B1	PROTEIN BINDING	341	275
H1151	A1B1	TRANSCRIPTION/Transferase	228	265
H1157	A1B1	OXIDOREDUCTASE	1524	265
H1166	A1B1C1	Unknown	577	175
H1167	A1B1C1	Unknown	560	275
H1168	A1B1C1	Unknown	567	175
T1109o	A2	Unknown	454	230
T1110o	A2	Unknown	454	200
T1113o	A2	VIRAL PROTEIN	386	415
T1121o	A2	DNA BINDING PROTEIN	762	250
T1123o	A2	VIRAL PROTEIN	532	215
T1124o	A2	TRANSFERASE	768	200
T1127o	A2	Unknown	422	235
T1132o	A6	CYTOSOLIC PROTEIN	612	230
T1153o	A2	Unknown	598	285
T1160o	A2	DNA BINDING PROTEIN	96	275
T1161o	A2	DNA BINDING PROTEIN	96	275
T1170o	A6	HYDROLASE	1908	97
T1173o	A3	CELL ADHESION	612	275
T1174o	A3	CELL ADHESION	1014	215
T1178o	A2	VIRAL PROTEIN	612	275
T1179o	A2	VIRAL PROTEIN	522	275
T1181o	A3	Unknown	2064	163
T1187o	A2	SUGAR BINDING PROTEIN	332	275

Table S2: Model quality distribution in terms of dockq_wave thresholds (bad: score < 0.23, acceptable: 0.23 <= score <0.49, good: 0.49 <= score) for CASP15_inhouse_dataset.

target	Number of bad models	Number of acceptable models	Number of good models
H1106	0	0	580
H1129	145	0	0
H1134	48	231	16
H1140	269	1	0
H1141	260	0	0
H1142	275	0	0
H1143	112	53	80
H1144	260	15	0
H1151	4	0	261
H1157	58	202	5
H1166	0	174	1
H1167	0	215	60
H1168	0	8	167
T1109o	1	189	40
T1110o	0	1	199
T1113o	9	0	406
T1121o	248	2	0
T1123o	95	118	2
T1124o	0	53	147
T1127o	4	12	219
T1132o	230	0	0
T1153o	98	2	185
T1160o	275	0	0
T1161o	275	0	0
T1170o	1	25	71
T1173o	181	67	27
T1174o	54	160	1
T1178o	25	116	134
T1179o	149	126	0
T1181o	162	1	0
T1187o	270	4	1

A.9 CASP15_community_dataset

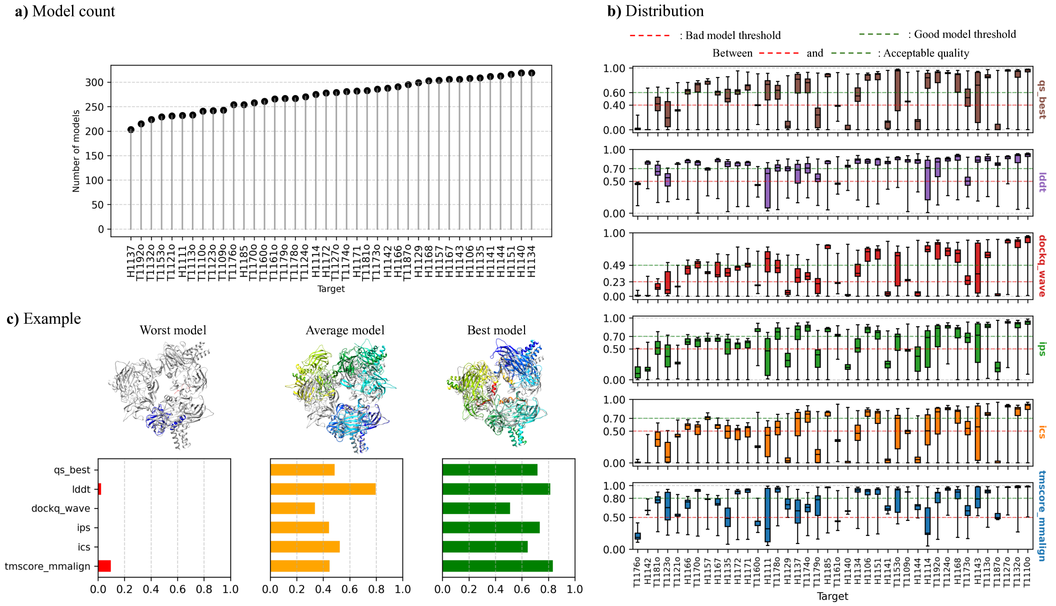

Figure S5: CASP15_community_dataset. (a) Model count. Number of models per target in the dataset. **(b) Score Distribution.** Box plots of each of six representative quality scores of the models for each target. **(c) Example.** Three representative models (worst, average, best) in terms of sum of the six representative quality scores for a target H1135. Each model with individual chains colored is superimposed with the true structure in gray.

Table S3: Summary of target information and the number of models per target in CASP15_community_dataset.

Target	Stoichiometry	Protein Classification	Seq. Length	Total models
H1106	A1B1	CHAPERONE	236	308
H1111	A9B9C9	PROTEIN TRANSPORT	8460	232
H1114	A4B8C8	OXIDOREDUCTASE	7988	275
H1129	A1B1	MEMBRANE PROTEIN	1387	299
H1134	A1B1	TOXIN/IMMUNE SYSTEM	543	319
H1135	A9B3	STRUCTURAL PROTEIN	1830	309
H1137	A1B1C1D1E1F1G2H1I1	MEMBRANE PROTEIN	4592	203
H1140	A1B1	PROTEIN BINDING	351	319
H1141	A1B1	PROTEIN BINDING	346	312
H1142	A1B1	PROTEIN BINDING	347	288
H1143	A1B1	PROTEIN BINDING	350	306
H1144	A1B1	PROTEIN BINDING	341	313
H1151	A1B1	TRANSCRIPTION/Transferase	228	316
H1157	A1B1	OXIDOREDUCTASE	1524	304
H1166	A1B1C1	Unknown	577	291
H1167	A1B1C1	Unknown	560	306
H1168	A1B1C1	Unknown	567	303
H1171	A6B1	HYDROLASE	1956	282
H1172	A6B2	HYDROLASE	2004	278
H1185	A1B1C1D1	DNA BINDING PROTEIN	1334	254
T1109o	A2	Unknown	454	243
T1110o	A2	Unknown	454	241
T1113o	A2	VIRAL PROTEIN	386	233
T1121o	A2	DNA BINDING PROTEIN	762	231
T1123o	A2	VIRAL PROTEIN	532	242
T1124o	A2	TRANSFERASE	768	270
T1127o	A2	Unknown	422	279
T1132o	A6	CYTOSOLIC PROTEIN	612	224
T1153o	A2	Unknown	598	229
T1160o	A2	DNA BINDING PROTEIN	96	261
T1161o	A2	DNA BINDING PROTEIN	96	266
T1170o	A6	HYDROLASE	1908	258
T1173o	A3	CELL ADHESION	612	286
T1174o	A3	CELL ADHESION	1014	281
T1176o	A8	UNKNOWN FUNCTION	1360	254
T1178o	A2	VIRAL PROTEIN	612	267
T1179o	A2	VIRAL PROTEIN	522	267
T1181o	A3	Unknown	2064	283
T1187o	A2	SUGAR BINDING PROTEIN	332	295
T1192o	A10	DNA BINDING PROTEIN	4180	215

Table S4: Model quality distribution in terms of dockq_wave thresholds (bad: score < 0.23, acceptable: 0.23 <= score < 0.49, good: 0.49 <= score) for CASP15_community_dataset.

Target	Number of bad models	Number of acceptable models	Number of good models
H1106	40	6	262
H1111	11	72	146
H1114	20	15	238
H1129	286	3	10
H1134	70	164	85
H1135	40	247	22
H1137	59	99	45
H1140	311	6	2
H1141	300	1	11
H1142	287	1	0
H1143	129	40	137
H1144	292	12	9
H1151	54	12	250
H1157	48	222	34
H1166	16	224	51
H1167	19	201	86
H1168	18	39	246
H1171	24	89	169
H1172	27	207	44
H1185	16	11	227
T1109o	37	187	19
T1110o	10	14	217
T1113o	25	7	201
T1121o	217	14	0
T1123o	155	78	9
T1124o	15	18	237
T1127o	8	8	263
T1132o	9	7	208
T1153o	68	16	145
T1160o	260	0	1
T1161o	259	4	3
T1170o	27	61	170
T1173o	133	114	39
T1174o	44	234	3
T1176o	254	0	0
T1178o	41	106	120
T1179o	171	86	10
T1181o	258	25	0
T1187o	272	5	18
T1192o	25	16	174

A.10 CASP16_inhouse_dataset

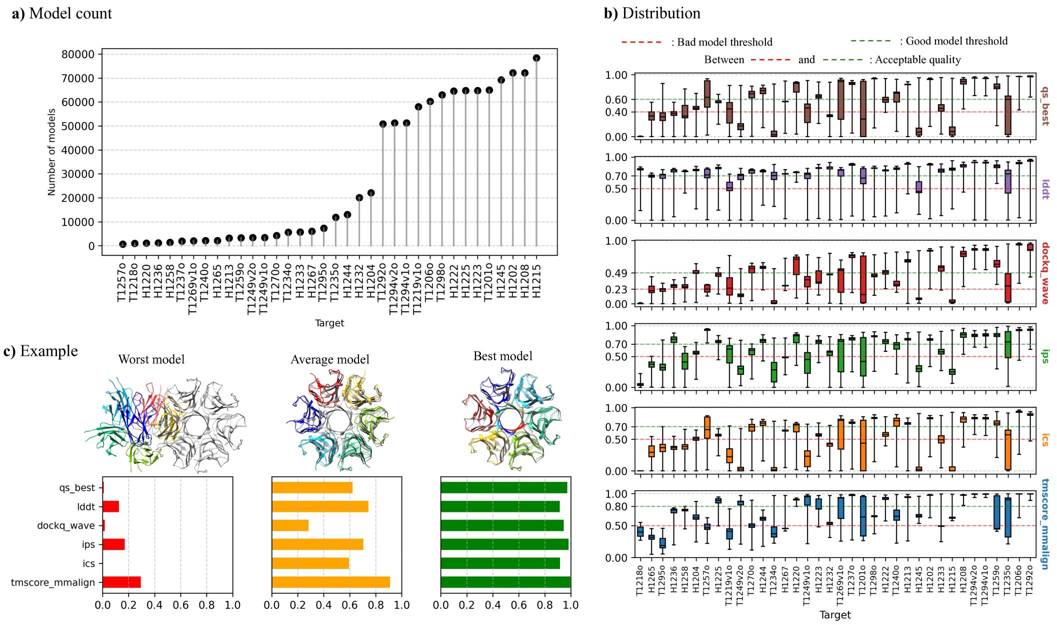

Figure S6: CASP16_inhouse_dataset. (a) Model count. Number of models per target in the dataset. **(b) Score Distribution.** Box plots of each of six representative quality scores of the models for each target. **(c) Example.** Three representative models (worst, average, best) in terms of sum of the six representative quality scores for a target T1235o. Each model with individual chains colored is superimposed with the true structure in gray.

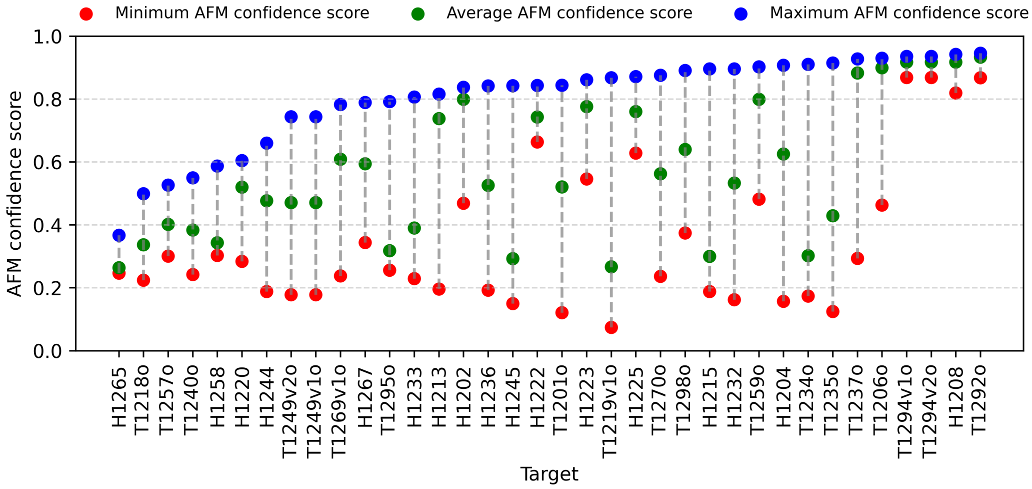

Figure S7: Distribution of AFM confidence scores of the structural models per target in CASP16_inhouse_dataset.

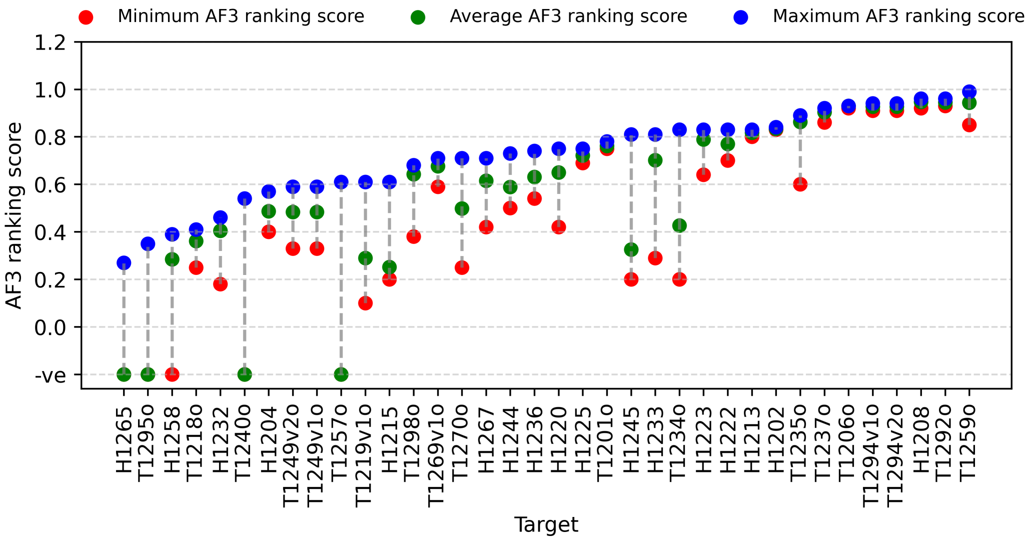

Figure S8: Distribution of AF3 ranking scores of the structural models per target in CASP16_inhouse_dataset.

Table S5: Summary of target information and number of models per target in CASP16_inhouse_dataset. It is worth noting that the length of three CASP16 targets (H1217, H1227, and H1272) exceeded the limit (about 5,000 residues) of running AlphaFold and required other structure prediction techniques such as template-based modeling. To make this dataset include only structural models generated by AlphaFold, they are excluded.

Target	Stoichiometry	Protein Classification	Seq. Length	Total models
H1202	A2B2	SIGNALING PROTEIN	380	72185
H1204	A2B2C2	OXYGEN TRANSPORT	858	22110
H1208	A1B1	Unknown	646	72200
H1213	A1B1C1D1E1	Unknown	1373	3200
H1215	A1B1	Unknown	369	78410
H1220	A1B4	Unknown	2515	1150
H1222	A1B1C1	Unknown	485	64600
H1223	A1B1C1	Unknown	486	64800
H1225	A1B1C1	Unknown	483	64799
H1232	A2B2	VIRAL PROTEIN	924	20090
H1233	A2B2C2	VIRAL PROTEIN/IMMUNE SYSTEM	1316	5700
H1236	A3B6	VIRUS	1929	1178
H1244	A2B2C2	Unknown	850	13000
H1245	A1B1	Unknown	317	69200
H1258	A1B2	Unknown	3092	1423
H1265	A9B18	Unknown	3924	2152
H1267	A2B2	Unknown	1852	6050
T1201o	A2	SIGNALING PROTEIN	420	65020
T1206o	A2	VIRAL PROTEIN	474	60205
T1218o	A2	Unknown	2328	949
T1219v1o	A10	Unknown	320	58000
T1234o	A3	VIRUS	1239	5600
T1235o	A6	VIRUS	690	11900
T1237o	A4	Unknown	1952	1970
T1240o	A3	Unknown	1959	2125
T1249v1o	A3	Unknown	1464	3450
T1249v2o	A3	Unknown	1464	3450
T1257o	A3	Unknown	3789	712
T1259o	A3	Unknown	729	3350
T1269v1o	A2	PROTEIN FIBRIL	2820	2025
T1270o	A6	Unknown	2622	4278
T1292o	A2	Unknown	392	50800
T1294v1o	A2	Unknown	428	51300
T1294v2o	A2	Unknown	428	51300
T1295o	A8	Unknown	3752	7369
T1298o	A2	Unknown	684	63000

Table S6: Model quality distribution in terms of dockq_wave scores (bad: score < 0.23, acceptable: 0.23 <= score < 0.49, good: 0.49 <= score) for CASP16_inhouse_dataset.

Target	Number of bad models	Number of acceptable models	Number of good models
H1202	0	448	71737
H1204	144	12112	9854
H1208	0	1135	71065
H1213	100	9	3091
H1215	77215	1024	171
H1220	16	505	629
H1222	0	25083	39517
H1223	84	47480	17236
H1225	20	46979	17800
H1232	26	18138	1926
H1233	2	883	4815
H1236	258	920	0
H1244	1	400	12599
H1245	66839	1682	679
H1258	252	1171	0
H1265	1279	873	0
H1267	1	6038	11
T1201o	34545	1227	29248
T1206o	0	1441	58764
T1218o	949	0	0
T1219v1o	25852	19207	12941
T1234o	5063	527	10
T1235o	5260	4097	2543
T1237o	2	29	1939
T1240o	80	2009	36
T1249v1o	803	2261	386
T1249v2o	3255	183	12
T1257o	352	360	0
T1259o	0	19	3331
T1269v1o	626	178	1221
T1270o	108	965	3205
T1292o	0	509	50291
T1294v1o	0	0	51300
T1294v2o	0	0	51300
T1295o	3668	3701	0
T1298o	1204	48835	12961

A.11 CASP16_community_dataset

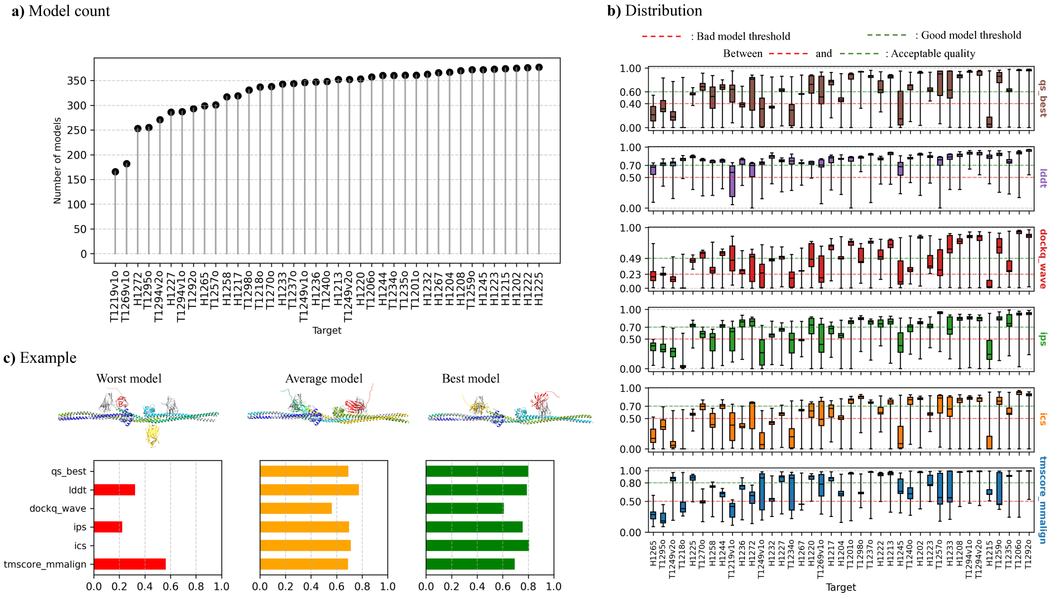

Figure S9: CASP16_community_dataset. (a) Model count. Number of models per target in the dataset. **(b) Score Distribution.** Box plots of each of six representative quality scores of the models for each target. **(c) Example.** Three representative models (worst, average, best) in terms of sum of the six representative quality scores for a target H1244. Each model with individual chains colored is superimposed with the true structure in gray.

Table S7: Summary of target information and number of models per target for CASP16_community_dataset.

Target	Stoichiometry	Protein Classification	Seq. Length	Total models
H1202	A2B2	SIGNALING PROTEIN	380	375
H1204	A2B2C2	OXYGEN TRANSPORT	858	367
H1208	A1B1	Unknown	646	370
H1213	A1B1C1D1E1	Unknown	1373	352
H1215	A1B1	Unknown	369	374
H1217	A2B2C2D2E2F2	Unknown	5878	319
H1220	A1B4	Unknown	2515	353
H1222	A1B1C1	Unknown	485	376
H1223	A1B1C1	Unknown	486	373
H1225	A1B1C1	Unknown	483	377
H1227	A1B6	Unknown	5689	286
H1232	A2B2	VIRAL PROTEIN	924	363
H1233	A2B2C2	VIRAL PROTEIN/IMMUNE SYSTEM	1316	343
H1236	A3B6	VIRUS	1929	347
H1244	A2B2C2	Unknown	850	360
H1245	A1B1	Unknown	317	372
H1258	A1B2	Unknown	3092	317
H1265	A9B18	Unknown	3924	299
H1267	A2B2	Unknown	1852	366
H1272	A1B1C1D1E1F1G1H1I1	MEMBRANE PROTEIN	6879	253
T1201o	A2	SIGNALING PROTEIN	420	361
T1206o	A2	VIRAL PROTEIN	474	357
T1218o	A2	Unknown	2328	337
T1219v1o	A10	Unknown	320	166
T1234o	A3	VIRUS	1239	360
T1235o	A6	VIRUS	690	361
T1237o	A4	Unknown	1952	344
T1240o	A3	Unknown	1959	348
T1249v1o	A3	Unknown	1464	346
T1249v2o	A3	Unknown	1464	352
T1257o	A3	Unknown	3789	301
T1259o	A3	Unknown	729	372
T1269v1o	A2	PROTEIN FIBRIL	2820	182
T1270o	A6	Unknown	2622	338
T1292o	A2	Unknown	392	293
T1294v1o	A2	Unknown	428	287
T1294v2o	A2	Unknown	428	271
T1295o	A8	Unknown	3752	255
T1298o	A2	Unknown	684	331

Table S8: Model quality distribution based on dockq_wave scores (bad: score < 0.23, acceptable: 0.23 <= score < 0.49, good: 0.49 <= score) for CASP16_community_dataset.

Target	Number of bad models	Number of acceptable models	Number of good models
H1202	2	37	336
H1204	21	176	170
H1208	31	15	324
H1213	33	16	303
H1215	333	12	29
H1217	1	13	305
H1220	13	174	166
H1222	2	102	272
H1223	0	239	134
H1225	0	289	88
H1227	5	86	195
H1232	25	263	75
H1233	12	35	296
H1236	86	255	6
H1244	39	15	306
H1245	204	104	64
H1258	53	262	2
H1265	208	86	5
H1267	31	331	4
H1272	69	33	151
T1201o	64	8	289
T1206o	27	30	300
T1218o	286	43	8
T1219v1o	32	52	82
T1234o	194	162	4
T1235o	52	238	71
T1237o	16	19	309
T1240o	22	321	5
T1249v1o	170	160	16
T1249v2o	303	46	3
T1257o	85	112	104
T1259o	11	9	352
T1269v1o	94	28	60
T1270o	22	57	259
T1292o	4	11	278
T1294v1o	4	3	280
T1294v2o	12	3	256
T1295o	117	138	0
T1298o	26	194	111

A.12 Multimer_7_2024_8_2025_dataset

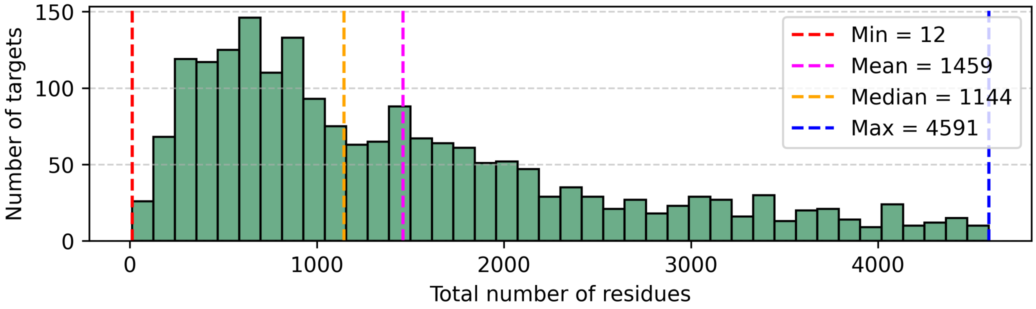

Figure S10: Distribution of residue count per target in Multimer_7_2024_8_2025_dataset.

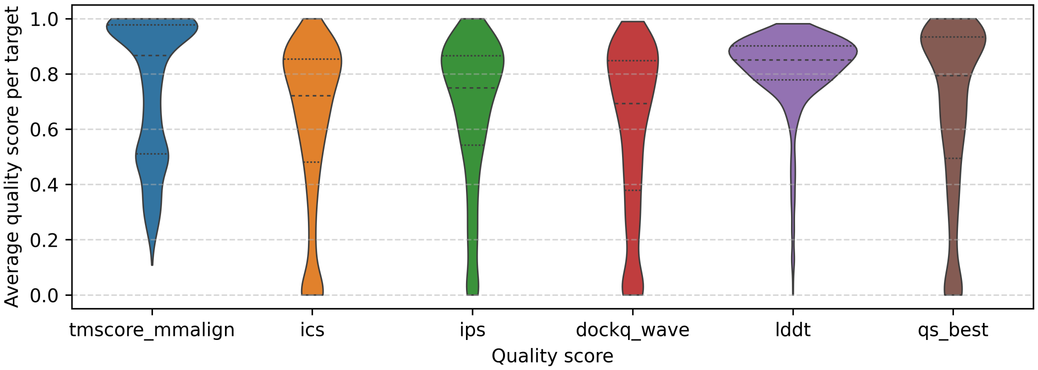

Figure S11: Violin plot of distribution of average quality scores of the structural models per target in Multimer_7_2024_8_2025_dataset.

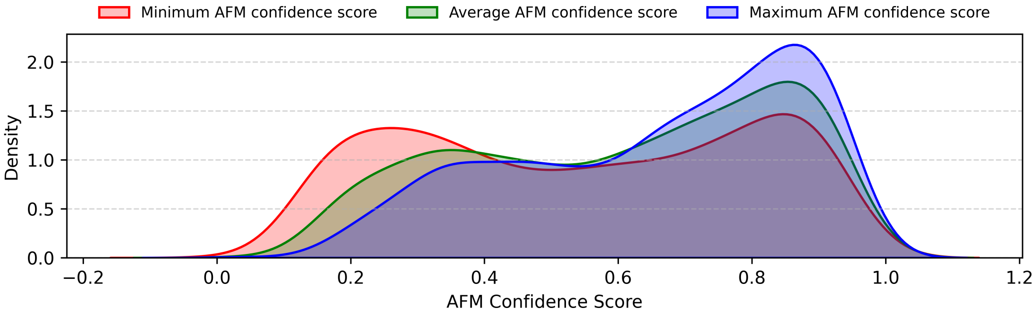

Figure S12: Density of AlphaFold-Multimer-style (AFM) confidence scores of the structural models per target in Multimer_7_2024_8_2025_dataset.

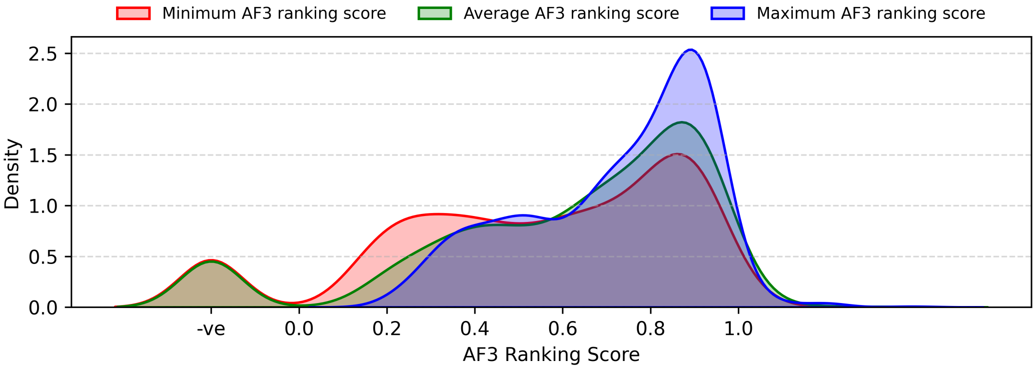

Figure S13: Density of AlphaFold3 (AF3) ranking scores of the structural models per target in Multimer_7_2024_8_2025_dataset.

A.13 CASP15_inhouse_TOP5_dataset and CASP16_inhouse_TOP5_dataset

CASP15_inhouse_TOP5_dataset and CASP16_inhouse_TOP5_dataset are the subset of CASP15_inhouse_dataset and CASP16_inhouse_dataset respectively. Each contains only top 5 models for each target predicted by each of dozens of AlphaFold-based predictors in our MULTICOM protein structure prediction system during CASP15 or CASP16, even though each predictor might generate many (e.g., hundreds of) models. These two subsets were used to train and evaluate GATE-AFM. The number of models per target in each of these two subsets is given in the Table S9.

Table S9: Summary of the CASP15 and CASP16 in-house TOP5 datasets.

CASP15_inhouse_TOP5_dataset		**CASP16_inhouse_TOP5_dataset**	
Target	Total Models	Target	Total Models
H1106	290	H1202	390
H1129	65	H1204	350
H1134	150	H1208	380
H1140	130	H1213	300
H1141	125	H1215	355
H1142	125	H1220	101
H1143	115	H1222	345
H1144	125	H1223	345
H1151	120	H1225	345
H1157	115	H1232	250
H1166	75	H1233	255
H1167	85	H1236	100
H1168	75	H1244	330
T1109o	115	H1245	360
T1110o	100	H1258	90
T1113o	210	H1265	77
T1121o	120	H1267	385
T1123o	110	T1201o	345
T1124o	100	T1206o	325
T1127o	120	T1218o	35
T1132o	115	T1219v1o	305
T1153o	130	T1234o	325
T1160o	125	T1235o	295
T1161o	125	T1237o	275
T1170o	45	T1240o	155
T1173o	125	T1257o	73
T1174o	95	T1259o	305
T1178o	125	T1269v1o	185
T1179o	125	T1270o	290
T1181o	65	T1292o	270
T1187o	125	T1295o	230
		T1298o	325

A.14 Analysis of Potential Bias from AlphaFold-Dominated Model Generation

An issue for PSBench is the potential bias introduced by the dominance of AlphaFold in model generation. Although the two community datasets (CASP15_community_dataset and CASP16_community_dataset) contain models from a variety of predictors, the majority of their models still originated from AlphaFold. The other three datasets in PSBench consist of AlphaFold-generated models only. This reflects the current landscape of protein structure prediction but may bias benchmark outcomes toward AlphaFold-specific characteristics.

To assess this bias, we compared TM-score distributions between the CASP community datasets (23,841 models from AlphaFold and non-AlphaFold predictors) and the AlphaFold-only in-house datasets. Community datasets exhibited a lower average TM-score (0.7166 vs. 0.7873) and a higher standard deviation (0.2394 vs. 0.2160), indicating slightly reduced average quality and greater variability compared to AlphaFold-only models.

We further examined the impact of this bias on EMA performance. Specifically, we compared GATE (trained on CASP15_community_dataset) and GATE-AFM (trained on CASP15_inhouse_TOP5_dataset) on the CASP16_inhouse_TOP5_dataset, which represents high-confidence AlphaFold predictions. As shown in Table S10 GATE-AFM outperformed GATE in

Spearman's correlation, loss, and AUROC for both TM-score and DockQ_Wave, while GATE achieved slightly higher Pearson's correlation on TM-score.

These results suggest that the training dataset composition can affect EMA generalization performance. We therefore caution users to consider model-generation bias when interpreting benchmark outcomes. We plan to incorporate models from emerging prediction methods in future PSBench releases to mitigate this bias.

Table S10: Performance of GATE-AFM and GATE on the CASP16_inhouse_TOP5_dataset. Metrics include Pearson's correlation (Corr^{P}), Spearman's correlation (Corr^{S}), ranking loss, and AUROC (75^{th} percentile cutoff) reported separately for TM-score and DockQ_wave. Bold values indicate better performance.

Method	TM-score				DockQ_wave			
	Corr^{P} ↑	Corr^{S} ↑	Loss ↓	AUROC ↑	Corr^{P} ↑	Corr^{S} ↑	Loss ↓	AUROC ↑
GATE-AFM	0.372	**0.283**	**0.102**	**0.658**	**0.431**	**0.322**	**0.138**	**0.662**
GATE	**0.408**	0.277	0.133	0.647	0.380	0.300	0.163	0.648

B Experimental Design

B.1 Standard EMA Methods in PSBench

PSBench includes six standard EMA methods that are publicly available. They serve as baseline methods for comparison with new EMA methods. Below is a brief overview of each method and its availability:

- **AlphaFold2-Multimer Confidence score (AFM Confidence)**[10]: AlphaFold2-Multimer provides self-estimated accuracy estimates for its predicted structures using a confidence score that is computed as a weighted sum of ipTM (interface predicted TM-score) and pTM (predicted TM-score), specifically: 0.8 * ipTM + 0.2 * pTM. This score serves as a single-model EMA method and a strong baseline for datasets generated by AlphaFold2-Multimer or AlphaFold3.
- **GATE**[18]: A multi-model EMA approach that leverages graph transformers applied to pairwise similarity graphs derived from input models. GATE combines both single-model and multi-model quality scores from individual models with comparative geometric similarities between models, enabling it to effectively predict the global structural accuracy (e.g., TM-score) of complex structural models. Source code is available at: `https://github.com/BioinfoMachineLearning/gate`. **GATE-AFM**: An enhanced variant of GATE by using AlphaFold2-Multimer features as additional node features. It can be used if such features are available.
- **DProQA**[31]: A single-model EMA method based on a Gated Graph Transformer architecture that modulates local neighborhood interactions. It is specifically designed to estimate the interface quality of protein complex models (e.g., DockQ scores) by leveraging a K-nearest neighbor (K-NN) graph representation of the complex structure. Source code is available at: `https://github.com/jianlin-cheng/DProQA`.
- **VoroMQA-dark, VoroIF-GNN-score, VoroIF-GNN-pCAD-score**[38]: A set of single-model EMA methods that utilize the VoroIF-GNN framework (Voronoi Interface Graph Neural Network) to assess protein complex interface quality. These methods operate on Voronoi tessellation-based atomic contact areas, capturing geometric and topological features of the interface. Source code is available at: `https://github.com/kliment-olechnovic/ftdmp`.
- **GCPNet-EMA**[39]: An EMA extension of GCPNet (Geometry-Complete Perceptron Network), a deep graph neural network that constructs a 3D graph representation from the atomic point cloud of a protein structure. It predicts both per-residue and per-model structural accuracy estimates, such as local and global lDDT. Although GCPNet-EMA is

originally trained on tertiary protein structures (e.g., single-chain models), it can be directly applied to evaluate the accuracy of protein complex structures. Source code is available at: https://github.com/BioinfoMachineLearning/GCPNet-EMA.

- **Average Pairwise Similarity Score (PSS)**[40]: A multi-model EMA method that evaluates each predicted complex by computing the average pairwise TM-score between it and all other models in the structural pool using MMalign. This simple yet effective consensus-based approach serves as a strong baseline for estimating the quality of the protein complex model. Source code is available at: https://github.com/BioinfoMachineLearning/MULTICOM_qa, with a simplified implementation available at: https://github.com/BioinfoMachineLearning/gate/blob/main/gate/feature/mmalign_pairwise.py.

It is worth noting that during benchmarking, the quality scores predicted by DProQA, VoroMQA and VoroIF-GNN, and GCPNet-EMA were normalized by multiplying the raw score by the ratio of the model length to the native structure length. This normalization penalizes shorter decoys, ensuring that the scores more accurately reflect both the completeness and the accuracy of the predicted models relative to the native structures.

B.2 The Details of Training and Validating GATE

GATE and GATE-AFM were first trained, validated, and tested on the CASP15 datasets (i.e., CASP15_community_dataset or CASP15_inhouse_dataset) respectively and then were blindly evaluated on unseen targets in the CASP16 datasets (i.e., CASP16_community_dataset or CASP16_inhouse_dataset) during the CASP16 competition from May to August, 2024.

Graph construction and architecture. To predict the quality scores for a set of complex structural models of a protein, GATE and GATE-AFM construct a pairwise model similarity graph in which each node represents a model, and an edge is formed between two nodes if the TM-score between the corresponding models exceeds 0.5. Each node is annotated with both single-model quality scores (e.g., ICPS, EnQA, DProQA, VoroMQA) and aggregated pairwise similarity scores (e.g., TM-score, QS-score, DockQ, CAD-score). For GATE-AFM, additional AlphaFold2-Multimer–specific features (confidence scores, ipTM, inter-chain predicted alignment errors, mpDockQ) are incorporated as node features. Edge features encode the pairwise similarity scores between connected models, including TM-score, QS-score, DockQ, and CAD-score.

From each full graph, 2,000–3,000 subgraphs are sampled, each containing up to 50 nodes. Within a subgraph, node and edge features are embedded, updated through graph transformer layers with multi-head attention and feed-forward networks, and passed through a multilayer perceptron (MLP) to predict a quality score for each node. The models are trained with a weighted loss combining a pointwise mean squared error (MSE) term (predicted vs. true scores) and a pairwise loss term (mean absolute error between predicted and true differences of model pairs). The pointwise loss weight was fixed at 1, while the pairwise loss weight was tuned as a hyperparameter.

Training protocol. GATE was trained and validated on the CASP15_community_dataset, which comprises 10,935 models of 40 protein targets, plus 187 models from another target (T1115o) whose native structure is not publicly available. For the 10,935 models, usalign_tmscore was used as labels. For T1115o, TM-scores were obtained from the CASP15 website. CASP15_community_dataset was partitioned into training, validation, and test sets using 10-fold cross-validation split by targets. For each target, 2,000 subgraphs were sampled, leading to 8,000–10,000 subgraphs per subset. Eight folds were used for training, one for validation, and one for testing, iterating across all folds. The fold assignments are listed in Table S11. Hyperparameter search space is shown in Table S12.

GATE-AFM. GATE-AFM was trained using the same cross-validation protocol and graph construction process as GATE, but on the CASP15_inhouse_TOP5_dataset (31 protein complex targets). To augment the data, 3,000 subgraphs per target were sampled. The only difference from GATE is that GATE-AFM incorporates AlphaFold2-Multimer–specific features as additional node features. TM-score labels were generated with an older version of the in-house TM-score script (tmscore_usalign_aligned_v0), which was later updated in CASP16 to correct minor alignment issues.

The updated version is included in PSBench, but the original scores remain available in the dataset to support reproducibility. The fold assignments are listed in Table S13.

Table S11: Targets assigned to each fold in the CASP15_community_dataset for training GATE.

Fold	Targets
Fold0	H1135, T1127o, T1161o, T1132o, H1144
Fold1	H1151, T1153o, H1171, H1114
Fold2	T1170o, H1166, T1176o, H1134
Fold3	H1111, H1106, T1109o, T1121o
Fold4	T1174o, T1115o, H1172, H1143
Fold5	H1137, H1142, T1192o, H1140
Fold6	T1187o, T1181o, T1179o, T1178o
Fold7	H1168, T1173o, T1160o, H1167
Fold8	T1113o, H1185, T1123o, H1157
Fold9	T1110o, H1141, T1124o, H1129

Table S12: Hyperparameter search space explored during model fine-tuning.

Hyperparameter	Candidate Values
Number of attention heads	4, 8
Number of graph transformer layers	2, 3, 4, 5
Dropout rate	0.1, 0.2, 0.3, 0.4, 0.5
MLP dropout rate	0.1, 0.2, 0.3, 0.4, 0.5
Hidden dimension	16, 32, 64
Weight of the pairwise MSE loss	`auto`, 0.01, 0.05, 0.1, 0.2, 0.3, 0.4, 0.5, 0.6, 0.7, 0.8, 0.9, 1
Optimizer	`AdamW`, `SGD`
Learning rate	1e-5, 5e-5, 1e-4, 5e-4, 1e-3
Weight decay	0.01, 0.05
Layer normalization	False, True
Batch size	256, 400, 512

Table S13: Targets assigned to each fold in the CASP15_inhouse_dataset for training GATE-AFM.

Fold	Targets
Fold0	T1127o, T1161o, T1132o, T1174o
Fold1	T1160o, H1106, H1134
Fold2	T1173o, T1178o, T1110o
Fold3	T1170o, H1142, H1140
Fold4	T1179o, T1187o, T1153o
Fold5	T1123o, H1151, T1181o
Fold6	T1121o, T1113o, H1144
Fold7	H1167, T1124o, H1157
Fold8	H1168, H1143, H1166
Fold9	H1141, T1109o, H1129

B.3 Computational Requirements for Training on PSBench

The computational cost of training EMA methods on the full PSBench dataset depends heavily on how structural models are used as inputs. For single-model EMA methods, where each model is processed independently, training time scales linearly with the number of models (e.g., 10,942 models in the CASP15_community_dataset). In contrast, multi-model methods such as GATE construct a pairwise model similarity graph for each target using all available models, which introduces quadratic or higher time complexity with respect to the number of models per target. However, once the similarity graph is constructed, extracting subgraphs and using them for training is considerably faster. Under this setup, GATE was trained using a single NVIDIA A100 GPU (80 GB) and required approximately 2 minutes per epoch. Researchers with smaller GPU memory may still train on PSBench by applying subgraph sampling or filtering strategies (e.g., using top-ranked models per target).

B.4 Threshold Selection for AUROC Evaluation

In the main experiments, we used the 75th percentile of the ground-truth scores (i.e., CASP official scores) for each target to define "high-quality" models in a relative sense. This percentile-based threshold adapts to the difficulty of individual targets and ensures balanced positive/negative class distribution for AUROC calculations across targets.

To assess the impact of threshold choice, we additionally evaluated AUROC using fixed cutoffs that are commonly used in the field. Specifically, we applied TM-score $\geq$ 0.5 and DockQ_Wave $\geq$ 0.49 to define high-quality models. Table S14 presents the performance of the EMA methods in PSBench under both percentile-based and fixed-threshold definitions on the CASP16_inhouse_TOP5_dataset. Under the fixed thresholds, GATE-AFM achieved AUROC scores of 0.635 (TM-score) and 0.684 (DockQ_Wave), which is ranked second among all the methods.

Statistical significance was assessed using a one-sided Wilcoxon signed-rank test comparing GATE-AFM with each baseline method. As indicated in Table S14, results marked with an asterisk (*) denote significant differences ($p < 0.05$). Under the fixed-threshold setting, GATE-AFM maintained strong performance and significantly outperformed most baseline methods, including AFM-Confidence, VoroIF-GNN, VoroIF-GNN-pCAD, and DProQA, across both TM-score and DockQ_Wave metrics. These results demonstrate that GATE-AFM remains one of the top-performing and statistically robust EMA methods, with consistent relative ranking and performance patterns regardless of the thresholding strategy.

Table S14: AUROC values of different EMA methods under 75th percentile and fixed threshold (0.5 and 0.49) definitions for TM-score and DockQ_Wave on CASP16_inhouse_TOP5_dataset. Significant difference ($p < 0.05$) between GATE-AFM and other methods based on the one-sided Wilcoxon signed-rank test is marked with *.

Methods	TM-score		DockQ_Wave	
	75th pct.	0.5 cutoff	75th pct.	0.49 cutoff
GATE-AFM	**0.658**	<u>0.635</u>	**0.662**	<u>0.684</u>
AFM-Confidence	0.597*	0.585*	0.593*	0.673
PSS	<u>0.647</u>	**0.650**	0.645	**0.685**
GCPNet-EMA	0.643	0.606*	<u>0.648</u>	0.672
VoroMQA-dark	0.609	0.570*	0.622	0.588*
VoroIF-GNN-pCAD	0.589*	0.541*	0.615	0.570*
VoroIF-GNN	0.599*	0.565*	0.622	0.601*
DProQA	0.569*	0.543*	0.587*	0.618

B.5 Failure Mode Analysis

To better understand the limitations of EMA methods, we examined failed cases (targets) with large prediction errors from GATE-AFM. Two recurring failure modes were identified.

For targets like H1202 and T1206o, EMA methods show high MAE (mean average error) despite the predicted models being generally good and similar. In these cases, GATE-AFM preserves relative rankings (low ranking loss) but underestimates absolute TM-scores, indicating a calibration issue. Its focus on pairwise relationships can compress score predictions, reducing absolute accuracy.

In contrast, H1265 includes only low-quality, diverse models with no resemblance to the native structure. Here, structural similarity among poor models misleads GATE-AFM, causing TM-score overestimation due to an uninformative similarity graph.

These cases reveal two distinct failure modes: score compression in high-quality model sets and misleading graph structures in poor-quality sets. By comparison, targets like H1215 and H1223, with varied and well-formed models, show low MAE and strong performance.

B.6 Ranking of EMA predictors on the CASP16_community_dataset based on Z-scores

To assess the overall performance of EMA predictors on the CASP16_community_dataset, we ranked the 38 EMA predictors based on cumulative positive Z-scores. For each target, the Z-scores for the predictors were computed separately for the four evaluation metrics (Pearson's correlation, Spearman's correlation, ranking loss, and AUROC) based on TM-score. The z-score for a predictor for a target is equal to the original score minus the average score of all the predictors divided by the standard deviation. When calculating total Z-scores for each predictor, only positive Z-scores for each target were accumulated to emphasize strong performances.

In this ranking, MULTICOM_GATE achieved third place with a total Z-score of 95.7, closely following ModFOLDdock2 (96.9) and MULTICOM_LLM (105.4).

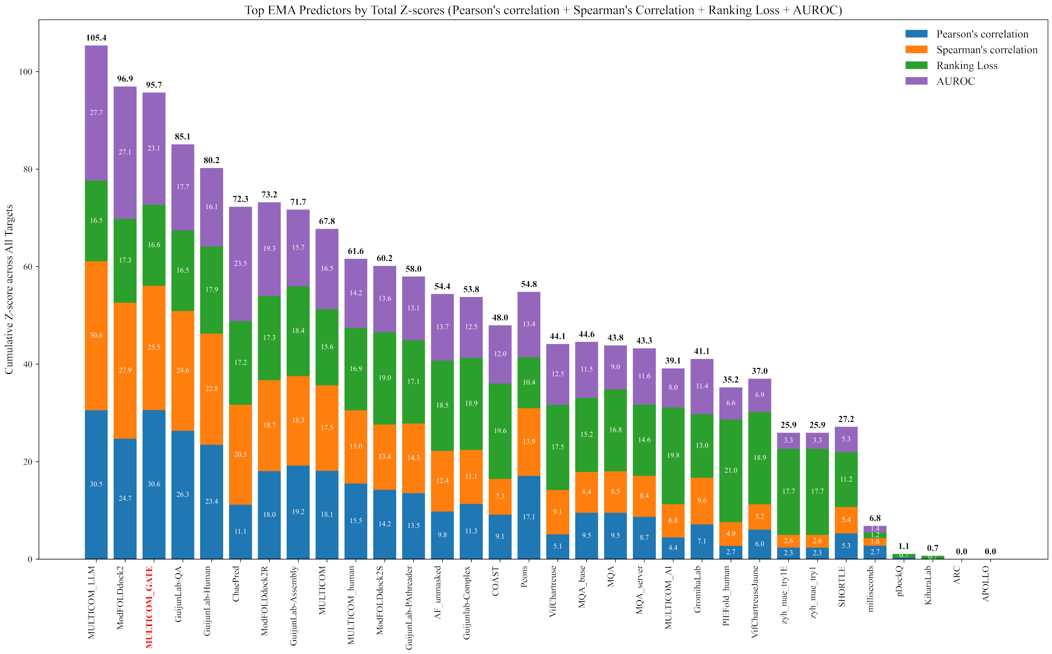

Figure S14: CASP16_community_dataset results. Stacked bar plot showing the cumulative positive Z-scores across all CASP16 community targets for the participated EMA predictors. Contributions from four performance metrics (Pearson's correlation, Spearman's correlation, ranking loss, and AUROC) are stacked to highlight the overall performance. EMA predictors are ranked by their total Z-scores. MULTICOM_GATE is colored in red.

B.7 Runtime and Memory Usage of EMA Methods

We compared the runtime and memory usage of representative EMA methods in PSBench on the computer system described in Appendix C.1. For GATE-AFM and GATE, the inference time after generating quality features for each model using external EMA methods is reported. Information for AFM-Confidence is not included since its estimates are generated alongside AlphaFold model predictions and are not obtained through a separate inference step.

Table S15 summarizes the results. Multi-model EMA methods such as GATE, GATE-AFM, and PSS generally provide higher predictive accuracy but require more memory and longer runtimes. In contrast, single-model methods such as GCPNet-EMA and DProQA are more lightweight but typically achieve lower accuracy. VoroMQAs were run on CPU in our experiments and therefore required longer runtimes compared to GCPNet-EMA or DProQA.

Table S15: Peak memory usage and runtime of EMA methods in PSBench.

EMA Method	CPU Mem (GB)	GPU Mem (GB)	Runtime (min)
GATE-AFM (inference)	100.9	11.9	12.98
GATE (inference)	100.1	12.0	31.04
PSS	0.53	N/A	18.88
GCPNet-EMA	0.53	0.64	11.13
VoroMQAs (CPU)	0.53	N/A	19.28
DProQA	0.53	2.63	4.72

C System Requirements

C.1 Environment for benchmarking EMA methods with PSBench and labeling model datasets

The generation of model quality scores and the evaluation of baseline EMA methods were performed on a computing server with the following specifications:

- **Operating System:** CentOS Linux
- **CPU:** AMD EPYC 7552, 3.2 GHz, 48 cores
- **RAM:** 50 GB
- **GPU:** NVIDIA A100, 80 GB (not required for quality score annotation, only needed to run some EMA methods)

C.2 Environment for training and validating GATE

The training and validation of the GATE and GATE-AFM were conducted on a high-performance computing system with the following configuration:

- **Operating System:** CentOS Linux
- **CPU:** AMD EPYC 7552, 3.2 GHz, 48 cores
- **RAM:** 500 GB
- **GPU:** NVIDIA A100, 80 GB